Ph.D. DISSERTATION

LOCALIZED VIRAL GENE DELIVERY USING ENCODED MICROPARTICLES FOR HIGH-THROUGHPUT HIGH-CONTENT CELL-BASED ASSAYS

고속 다중변수 세포기반 분석을 위한
코드화된 미세입자를 이용한
지역화된 바이러스 기반의 유전자 전달

BY

SANGKWON HAN

AUGUST 2015

DEPARTMENT OF ELECTRICAL ENGINEERING AND
COMPUTER SCIENCE
COLLEGE OF ENGINEERING
SEOUL NATIONAL UNIVERSITY

Ph.D. DISSERTATION

LOCALIZED VIRAL GENE DELIVERY USING ENCODED MICROPARTICLES FOR HIGH-THROUGHPUT HIGH-CONTENT CELL-BASED ASSAYS

고속 다중변수 세포기반 분석을 위한
코드화된 미세입자를 이용한
지역화된 바이러스 기반의 유전자 전달

BY

SANGKWON HAN

AUGUST 2015

DEPARTMENT OF ELECTRICAL ENGINEERING AND
COMPUTER SCIENCE
COLLEGE OF ENGINEERING
SEOUL NATIONAL UNIVERSITY

LOCALIZED VIRAL GENE DELIVERY USING ENCODED MICROPARTICLES FOR HIGH-THROUGHPUT HIGH-CONTENT CELL-BASED ASSAYS

고속 다중변수 세포기반 분석을 위한 코드화된 미세입자를 이용한 지역화된 바이러스 기반의 유전자 전달

지도교수 권 성 훈

이 논문을 공학박사 학위논문으로 제출함

2015 년 6 월

서울대학교 대학원

전기컴퓨터 공학부

한 상 권

한상권의 공학박사 학위논문을 인준함

2015 년 6 월

위 원 장 : 박 영 준

부위원장 : 권 성 훈

위 원 : 신 영 기

위 원 : 김 성 재

위 원 : Helene Andersson Svahn

Abstract

In this dissertation, I develop an adenoviral vector-immobilised patch-type encoded microparticle for high-throughput, high-content cellular assays and name this 'encoded viral micropatch'. This technology spatially confines the adenoviral gene delivery to only the cells under the micropatch by simply pipetting a heterogeneous mixture of the two-dimensional (2D) shape-coded viral micropatches on monolayer-cultured cells. Distinct clusters of transduced cells are then created in correspondence with the randomly positioned micropatches and the delivered gene into the cells within each cluster can be identified using the shape of the micropatch. For this purpose, shape-coded polymer microparticles are fabricated by photolithography, and highly localized gene delivery is achieved by specifically immobilizing adenoviral vectors on the microparticles. This unique feature allows high-throughput compound screening by virtue of multiplexing in a well of a standard microplate and creates no restriction for fluorescence-based assay formats

with high-content imagers. To highlight the capabilities of this technology, I demonstrate a multiplex G-protein coupled receptor (GPCR) internalization assay that requires compound treatments followed by fluorescence-based target tracking at the sub-cellular level.

First, I develop the maskless lithography system supporting an automated step-and-repeat operation for the fabrication of microparticles with various 2D graphical codes. Using this system, I explore new applications of the encoded microparticles and lithography technique such as anti-counterfeiting of drugs, parallel loading of small volume liquid for multiplexed bioassays, and conformal phosphor coating for white light-emitting diodes (LEDs).

For the development of the encoded viral micropatch, various shape-coded microparticles are fabricated with carboxyl groups on the surfaces for specific immobilization of adenoviral vectors. The chemical functionalization is achieved by the incorporation of acrylic acid to photocurable polymer solution. Then, two adenoviral vector immobilization methods are developed with this shape-coded microparticle. The first method is to directly link the carboxyl groups on the microparticle and the primary amine groups on the surface proteins of adenoviral vectors using 1-ethyl-3-(3-dimethylaminopropyl)carbodiimide (EDC) plus N-hydroxysulfosuccinimide (Sulfo-NHS) crosslinking reaction. The immobilization of adenoviral vectors in this approach is confirmed by an immunofluorescence test and

a scanning electron microscope (SEM) observation. The second method utilizes an avidin-biotin interaction. In this approach, both the microparticles and adenoviral vectors are biotinylated using amine-activated and amine-reactive biotin reagents, respectively. Then, they are linked by the mediation of avidin. The immobilized adenoviral vectors are well observed using a SEM.

The localized viral gene delivery of two types of the encoded viral micropatches is evaluated by transducing a human osteosarcoma cell line (U-2 OS) cultured in a standard 96-well microtiter plate. The first type of the encoded viral micropatch fabricated via EDC/Sulfo-NHS reaction shows low rate of the localization of gene delivery due to an escape of non-specifically bound adenoviral vectors. However, the second type of the encoded viral micropatch fabricated utilizing avidin-biotin interaction offers highly localized gene delivery. This is owing to the viral receptor-independent transduction of the biotinylated adenoviral vector, which is further supported by the transduction experiment of an adenovirus receptor-deficient cell line.

Finally, I demonstrate a multiplexed GPCR internalization assay based on the localized gene delivery with the encoded viral micropatches. The development of high-throughput cell-based GPCR functional assays is very important for screening large compound libraries in the drug discovery process and ligand-induced receptor internalization assays have broad applicability to various GPCR subfamilies among

several GPCR assay formats. However, high-content imaging is required for fluorescence-based intracellular measurement of receptor internalization. To address this issue, I fabricate three types of encoded viral micropatches with adenoviral vectors bearing green fluorescence protein (GFP)-tagged GPCR genes. Then, the responses of multiple GPCRs against one ligand treatment is acquired in one reaction site by achieving simultaneous expression of multiple GPCRs with the fabricated viral micropatches in a cell monolayer cultured in a well of a 96-well plate. High-content analysis of this micropatch-based multiplexed assay shows comparable results in the receptor internalization with the conventional singlet assay using free adenoviral vectors while reducing the number of pipetting actions.

Keywords: Cell-based assays, High-content screening, Multiplexing, Viral gene delivery, Encoded microparticle

Student Number: 2010-20910

Contents

List of Figures

List of Tables

Chapter 1

Introduction

In this dissertation, I present a new encoded micropaticle-mediated adenoviral gene delivery method that simultaneously supports high-throughput and high-content cell-based assays. This technology delivers multiple types of genes to monolayer-cultured cells with a spatial confinement by a single pipetting of a heterogeneous mixture of the 2D shape-coded and viral vector-immobilized microparticles. Thus, it allows high-throughput compound screening by virtue of multiplexing in a well of a standard microplate and created no restriction for fluorescence-based assay formats with high-content imagers.

In chapter 1, I describe the importance of cell-based assays in drug discovery process. Especially, high-content screening and cell microarray technology are introduced because the study in this dissertation aims the conveniently configurable

cell microarray compatible with image-based high-content screening. Lastly, the main concept of this research that utilizes adenoviral vector immobilization on encoded microparticles and their patch-type use on a cell layer is described and named ‘encoded viral micropatch’.

In chapter 2, the development of the encoded viral micropatch is introduced including encoded microparticle fabrication and adenoviral vector immobilization. Maskless lithography system with an automated step-and-repeat operation is firstly developed for the mass production of microparticles with various 2D graphical codes. For the encoded viral micropatch, shape-coded microparticles are fabricated with the surface functionalization. Then, two strategies are applied for the immobilization of adenoviral vectors on the microparticles; one is to directly conjugate the chemical functional groups on the microparticles and the surface proteins of adenoviral vectors via a carbodiimide crosslinker (type 1 encoded viral micropatch). The other is to apply biotin conjugation on both the microparticles and adenoviral vectors followed by avidin-mediated link of them (type 2 encoded viral micropatch). The adenoviral immobilization in each method is confirmed by an immunofluorescence test and/or a scanning electron microscope observation.

In chapter 3, the localized gene delivery of both types of the encoded viral micropatch is evaluated. The encoded viral micropatches are fabricated with adenoviral vectors carrying fluorescence protein genes. Quantitative analysis of the

expression of fluorescence proteins in cells under and outside the miropatch reveals that the type 2 encoded viral micropatch offers highly localized gene delivery. The reason of the highly localized gene delivery is further investigated and utilized for transducing an adenovirus receptor-deficient cell line. Lastly, the number of the immobilized adenoviral vectors is measured by quantifying a viral DNA to study the transduction efficiency of the type 2 encoded viral micropatch.

In chapter 4, a multiplex GPCR internalization assay is demonstrated in high-content manner to highlight the capability of this technology. Three types of encoded viral micropatches with adenoviral vectors bearing GFP-tagged GPCR genes (Ad-GPCR-GFP) are fabricated and simultaneous expression of multiple GPCRs in one reaction site is achieved by a single pipetting of a mixture of the fabricated Ad-GPCR-GFP micropatches. Thus, the response of multiple GPCRs against one ligand is acquired from a single well in 96-well microtiter plate. Also, high-content analysis of this micropatch-based multiplexed assay shows that it gives comparable results with a conventional singlet assay using free adenoviral vectors.

I envision that the encoded viral micropatch greatly simplifies the construction of cell microarray and offers the compatibility with high-content imagers, thus accelerating and enriching cell-based assay for drug discovery.

1.1 Cell-based Assays in Drug Discovery

The journey from drug discovery to commercialization is lengthy and expensive [1]. It usually takes over 10 years and costs approximately a billion dollars with over a thousand of testing on animals and humans to obtain clinical approval. Although tremendous amount of money and time as well as human resources are investigated in drug discovery process, it has very low success rate of finding a new drug. Drug discovery process starts with a million compounds and on average, approximately 250 lead compounds enter pre-clinical testing, 5 of them proceed to clinical trials, and only one chemical entities are approved by the US Food and Drug Administration (FDA) as depicted in figure 1.1. Therefore, in order to increase the productivity of drug screening, it is important to obtain biologically relevant information about activity, mechanism, toxicity, and side effect of drug candidate lead compounds in the early stages of drug discovery.

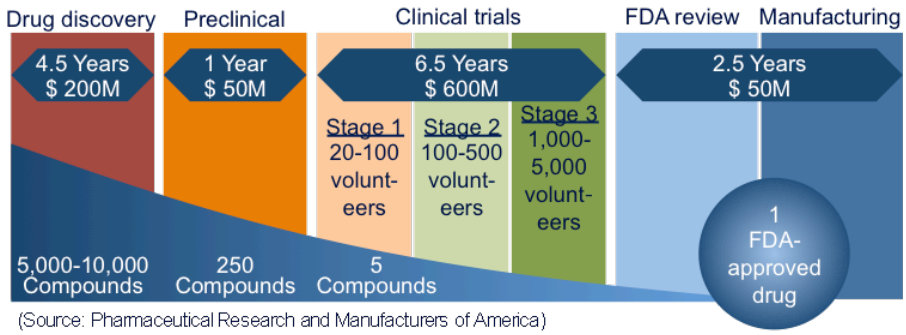

Figure 1.1 The journey from drug discovery to commercialization.

The early stages of the drug discovery process have relied on target-based biochemical assays, which include examination of enzyme activity, receptor-ligand binding, or protein-protein interactions [2]. In a biochemical assay, targets of interest are purified and prepared to test direct and specific binding of compounds. However, not all targets can be purified or prepared in a manner suitable for biochemical measurement. Furthermore, drug responses in a biochemical assay cannot precisely represent *in vivo* or tissue specific responses due to the absence of cellular co-factors, and the ability to examine off-target effects and cytotoxicity.

Cell-based assays, on the other hand, measure a variety of responses of living cells including cell proliferation, motility, morphological changes, toxicity, production of markers, and activation of specific signaling pathways [3]. Due to its capacity to predict *in vivo* effects, the majority of assays used for target identification and compound screening for drug discovery are employing cell-based assays and pharmaceutical companies are gradually replacing biochemical assays with cell-based assays in drug discovery.

Cell-based assays in drug discovery are commonly conducted within gain-of-function experiments by over-expression of target genes or by loss-of-function experiments via silencing of genes [4]. In these cellular assays, the expression of target proteins is essential for analyzing their phenotypic roles and intracellular redistribution initiated by compound treatments. Historically, stable cell line have

been the main stay of these cell-based assays [5]. However, because generation of cell lines that readily express target proteins without decrease of expression level is very challenge and, more importantly, the number and diversity of potential drug target have been rapidly increased, cell-based assays have adopted transient expression of target proteins. In this regard, viral gene delivery systems have gained prominence for transient target gene expression in cell-based assays to avoid the challenges associated with the development of cell lines that stably express target proteins [5, 6]. Viral vectors have high delivery efficiency to a broad range of cell types and also offer flexibility for expression modulation. These advantages make viral-mediated gene delivery favorable to cell-based target validation and compound screening for drug discovery [6].

In the past, cell-based assays were slow and expensive, and lacked reproducibility. However, cell-based assays are becoming faster, cheaper, and more reproducible as new technologies appear. Subsequently, a desire to increase the amount and quality of information obtained from cell-based assays has emerged [7]. One approach to meet this desire is to obtain multiple data from a single assay. There are two ways for achieving this purpose: multi-parametric assays and multiplexed assays. Multi-parametric assays are defined as those yielding multiple measurements from a single cell type and multiplexed assays are defined as those producing a single measurement for multiple cell types with a single environement.

1.2 Image-based High-content Screening

Cell-based assays for drug screening fall into three main categories: second messenger assays that monitor signal transduction following activation of cell-surface receptors, reporter gene assays that monitor cellular responses at the transcription/translation level, and cell proliferation assays that monitor the overall cell growth or death in response to external stimuli or stress [8]. The examples of each assay type are summarized in table 1.1.

Table 1.1 Major types of cell-based assays used for drug screening [1].

Assay type	Examples
Second messenger	Using fluorescent molecules that respond to changes in intracellular Ca^{2+} concentration, membrane potential, pH, etc. to assay receptor stimulation and ion channel activation [9, 10]
Reporter gene	Co-expression of luciferase to catalyze the light-emitting luciferin reaction for detection of protein kinase C inhibitors [11, 12]
Cell proliferation/toxicity	Virus-induced cytopathic effects on cell proliferation monitored by following the reduction of tetrazolium salt to formazan quantified by absorbance at 410 nm [13]

These types of cell-based assays are extensively applied in drug discovery programs performed by pharmaceutical industry. One limitation of these assays is that they provide information about a single parameter only. Thus, multi-parametric approach with sub-cellular imaging has recently attracted great attention of many researchers who run cell-based assays in order to increase the amount and quality of information obtained from their screening assays.

Image-based cellular assays, often referred to as high-content screening (HCS), are becoming important tools for increasing the amount and quality of data generated from cell-based assays [14-16]. These assays typically use automated, high-resolution fluorescence microscopy platforms to analyze cells with multiple parameters like shape and size of cytoplasm and nucleus as well as target-specific fluorescence readouts. These parameters can deliver various insights of the compound's mode of action and unspecific effects early on [17].

In addition to increased content, HCS also enables analysis of trafficking or intracellular redistribution of proteins within cells or morphological changes by sophisticated and quantitative analysis of sub-cellular images. Microscopic analyses can also performed in living cells for extended periods of time and thus enable kinetic analysis of cellular/intracellular activities or the order of occurrence of phenotypes during the observation period [18]. These benefits of HCS provide more information than the traditional screenings.

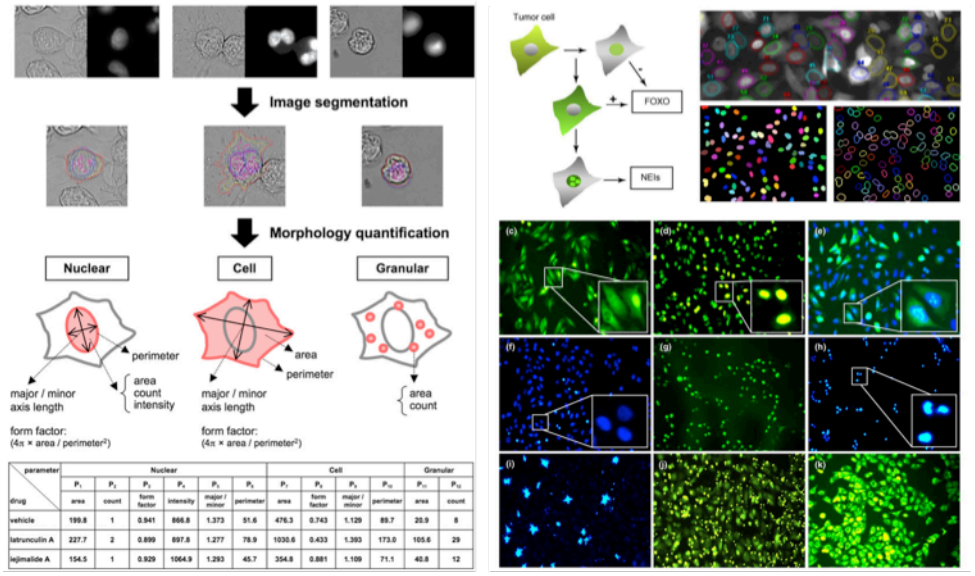

parameter / drug	Nuclear						Cell				Granular	
	P_1 area	P_2 count	P_3 form factor	P_4 intensity	P_5 major / minor	P_6 perimeter	P_7 area	P_8 form factor	P_9 major / minor	P_{10} perimeter	P_{11} area	P_{12} count
vehicle	199.8	1	0.941	866.8	1.373	51.6	476.3	0.743	1.129	89.7	20.9	8
latrunculin A	227.7	2	0.899	897.8	1.277	78.9	1030.6	0.433	1.393	173.0	105.6	29
iejimalide A	154.5	1	0.929	1064.9	1.293	45.7	354.8	0.881	1.109	71.1	40.8	12

Figure 1.2 Examples of high-content screening including multi-parametric analysis of cell physiology and intracellular location of protein [16, 19].

1.3 Cell Microarray for High-throughput Screening

Multiplexing, defined as the simultaneous screening of multiple targets in the same experiment, provides new potential for cell-based assays [7]. It allows not only parallel examination of compound activity against multiple targets but also efficient execution of compound selectivity test early in the drug discovery process. In addition, the quality of screening data is improved by removing uncertainty regarding pipetting errors and by including controls in the same environment. One efficient way for achieving the multiplex cell-based assays is to spatially localize the expression of target proteins using transient gene delivery.

As I mentioned in previous section, viral vectors are increasingly being used for transient target protein expression in cell-based assays. Basically, viral vectors are delivered to cells in the form of nanoparticle suspension and once bound to their specific receptors, viruses enter the cells to deliver the gene. Therefore, in order to spatially confine viral gene delivery, they should be immobilized on a substrate on which cells will grow. Planar microarrays of viral vectors have been developed utilising robotic spotting of viral solutions on glass slides for high-throughput gene function studies [20-23]. After cells are seeded on the slide, viral transduction occurs locally on the viral spots, thus creating an array of cells expressing distinct target proteins (figure 1.3). Because they can have at least 5,000–6,000 spots on one slide, the throughput of assays is significantly increased. In addition, cell microarrays

reduce the cost of each experiment because small amount of expensive reagents and biological samples are needed by virtue of extreme miniaturization of assays [24]. Thus, cell microarrays hold great potential in the field of drug discovery.

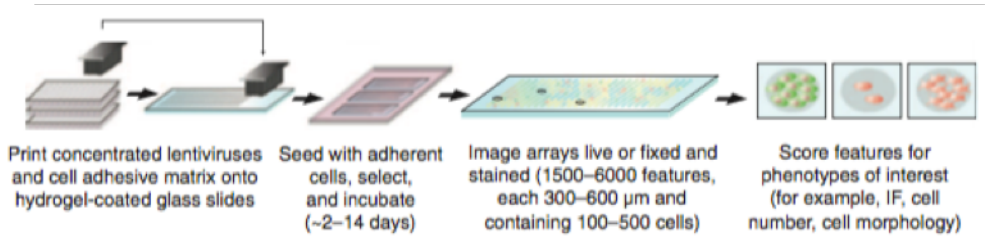

Figure 1.3 Cell microarray platform using robotic spotting of viral solutions on a glass slide [23].

1.4 Main Concept: Encoded Viral Micropatch

Functional analysis of many genes can be performed in parallel in high-density viral microarrays. However, planar viral microarrays are unsuitable for high-throughput screening of large libraries of compounds. An array of cells sharing a common medium on a centimetre-sized glass slide can be treated with only one compound unless special devices are used to separate the spots into chambers on the glass slide [25]. In addition, planar array technologies suffer from low productivity with limited number of spots that can be produced at the same time and, more importantly, the spots cannot be tested to assure the quality. Users are also forced to order an array with a predetermined panel of viral spots for every single assay [26, 27].

Encoded microparticles, on the other hand, can be used for localized viral gene delivery to construct an easily scalable and configurable suspension viral microarray by just mixing different viral vector-immobilized microparticles produced in bulk and quality-controlled by sampling test. Recently, an encoded microsphere was evaluated as a cell carrier that allows viral transduction of cells for potential use in multiplex cell-based assays [28]. An identification code was photophysically written on the surface of microsphere and adenoviral vectors were electrostatically immobilized. Through agitation culture with the microsphere, only cells grown on the microspheres became transduced. However, neither viral gene delivery nor cell-based assays have been yet demonstrated in multiplex format using this technology.

Furthermore, this format is severely incompatible with high-content screening. The different focal planes of cells on the microsphere restrict sub-cellular imaging with high-resolution microscopes and fluorescence-based encoding of the microsphere narrows the use of fluorescent dyes or protein markers to detect the cellular contents.

In this dissertation, I develop an adenoviral vector-immobilized patch-type encoded microparticle for high-throughput, high-content cellular assays and name this 'encoded viral micropatch'. This technology spatially confines the adenoviral gene delivery to only the cells under the micropatch by pipetting a heterogeneous mixture of the 2D shape-coded viral micropatches on monolayer-cultured cells. Distinct clusters of transduced cells are then created in correspondence with the randomly positioned micropatches and the delivered gene into the cells within each cluster can be identified using the shape of the micropatch (figure. 1.4). For this purpose, shape-coded polymer microparticles are fabricated by photolithography, and highly localized gene delivery is achieved by specifically immobilizing adenoviral vectors on the microparticles. This unique feature allows high-throughput compound screening by virtue of multiplexing in a well of a standard microplate and creates no restriction for fluorescence-based assay formats with high-content imagers. To highlight the capabilities of this approach, I demonstrate a multiplex GPCR internalization assay that requires compound treatments followed by fluorescence-based target tracking at the sub-cellular level.

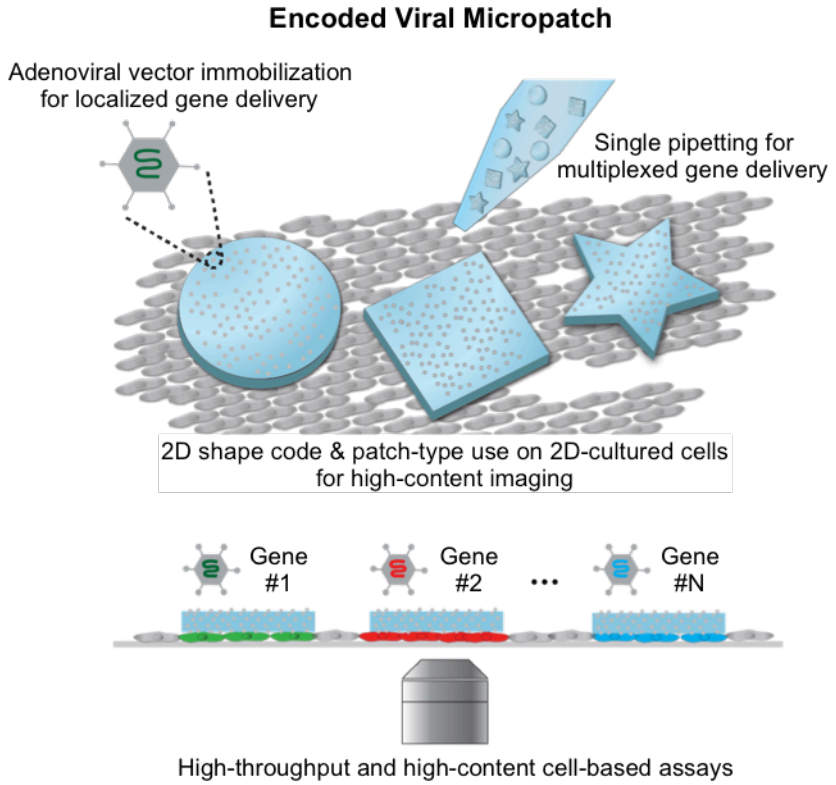

Figure 1.4 Encoded viral micropatch for localized adenoviral gene delivery and high-content screening. The patch-type use on a 2D cell layer and 2D shape encoding not only enable the spatial confinement of adenoviral gene delivery but also provide high compatibility with fluorescence-based high-content imaging system.

Chapter 2

Development of Encoded Viral Micropatch

In this chapter, I introduce fabrication methods of the encoded viral micropatch consisting of encoded microparticle fabrication and adenoviral vector immobilization. First, the fabrication of encoded microparticles with a 2D graphical code using a maskless lithography system is described. Then, I introduce two strategies of adenoviral vector immobilization on the encoded microparticles.

2.1 Introduction

In order to develop the encoded viral micropatch, encoded microparticles with a large number of distinct identification codes should be easily fabricated to deal with diverse transgenes and the surface of the microparticle should have functional groups to specifically immobilize viral vectors. Photopolymerization techniques are suitable for achieving these two features [29-32]. By exposing photocurable oligomer liquid to patterned light, microparticles can be fabricated with precisely controlled shapes or patterns. In addition, the fabricated microparticles can have chemically reactive moieties on their surfaces by simply adding proper materials to oligomer liquid. In conventional optical projection lithography system, a photomask is used to define the pattern of light. However, it's not feasible to manage a large number of codes on a photomask basis in terms of cost and cycle time. In order to overcome these limitations, maskless lithography systems have been developed [33-36]. They typically use computer-controlled programmable micromirror spatial light modulators (SLMs) instead of traditional photomasks, thus removing cost and time for creating and applying a new photomask with each design change. For this reason, I will use maskless lithography system to fabricate encoded microparticles for the encoded viral micropatch.

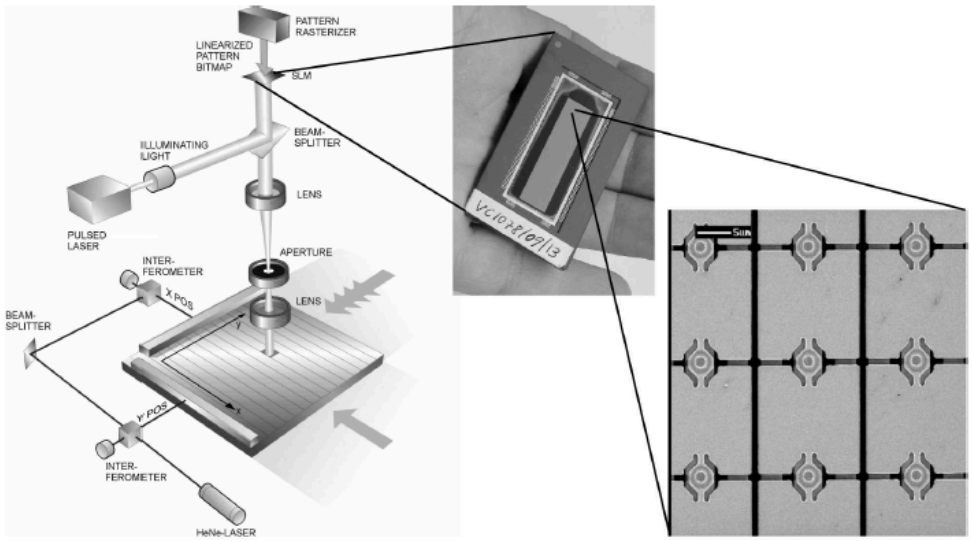

Figure 2.1 Principle of operation of an optical maskless tool using SLMs [33].

Another main step for the development of encoded viral micropatch is viral vector immobilization on the encoded microparticles. Viral vectors are increasingly being used for target protein expression in cell-based assays because they provide high transduction efficiencies to a broad range of cell types [5, 37, 38]. Basically, viral vectors are delivered to cells in the form of viral particle suspension and once bound to their specific receptors, viruses enter the cells to deliver the gene [39]. Therefore, in order to spatially confine viral gene delivery, they should be immobilized on a solid support. The immobilization methods can be categorized into non-specific and specific binding. Non-specific binding includes electrostatic, van der Waals, and hydrophobic interactions. Specific binding utilizes the interactions of functional groups on viral capsid and substrate surfaces. In general, specific binding

approaches more effectively prevent unwanted release of viral vectors and results in-site-specific delivery [40]. Because this is more beneficial to localized gene delivery, I will develop specific binding method for viral vector immobilization on the encoded microparticles.

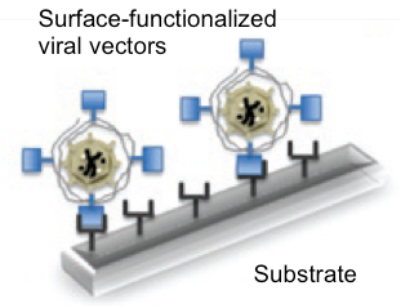

Figure 2.2 Schematic illustrating specific binding of surface-functionalized viral vectors on a substrate [40].

2.2 Fabrication of Encoded Microparticles

2.2.1 Maskless Lithography System

An optofluidic maskless lithography (OFML) system has been developed in our research group for synthesis of free-floating microstructures with various 2D shapes in microfluidic channels [34]. It is composed of a microfluidic device and an optical lithography system (figure 2.3a). Ultravirolet (UV) light, reflected off arbitrary patterns on a digital micromirror device (DMD) is projected onto a photocurable polymer solution in a microfluidic channel. By controlling the patterns on the DMD in real-time with precise flow control in the microfluidic channel, polymeric microstructures can be continuously fabricated with dynamic changes of their shapes (figure 2.3b).

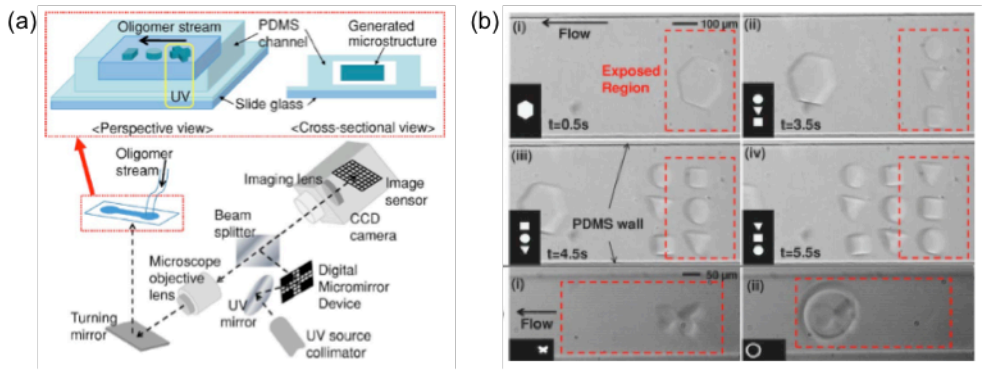

Figure 2.3 Optofluidic maskless lithography (OFML) system [34]: (a) schematic diagram of the system; (b) continuous fabrication of free-floating microstructures with various shapes in a microfluidic channel.

However, there are several practical problems to use this flow lithography for mass production of microparticles. In OFML system, photocurable polymer solutions should flow to take the fabricated microstructures and to allow synthesis of new structures at the same location because the exposure area of UV light is fixed. However, this operation requires external devices such as pneumatic pumps and valves to actively push and stop the flow. More importantly, this flow control should be adjusted according to mechanical and chemical properties of polymer solutions in order to obtain high contrast features. In addition, after repetitive photopolymerization at the same location, polymerized microstructures start to stick to the bottom of the microfluidic channel because of loss of oxygen inhibition layer [41]. Thus, the number of microparticles that can be fabricated in one microfluidic channel is severely limited.

To address this issue, I develop a maskless lithography system providing a step-and-repeat operation without flow control in a microfluidic channel (figure 2.4). Instead of using a microfluidic channel, photocurable polymer solution is prepared as sandwiched between two glass slides. The gap of two glass slides created by thin spacers determines the height of microparticle. A motorized stage (SCAN IM 112×74, MÄRZHÄUSER WETZLAR, Germany), on which the sandwiched glass slides are placed, is equipped to make whole area of a glass slide exposed to UV light (LC8, Hamamatsu, Japan) in an automated step-and-repeat manner. In order to

implement the automated step-and-repeat lithography operation, all components including a UV light source, a DMD, and a motorized stage are controlled in a unified manner by a home-grown software.

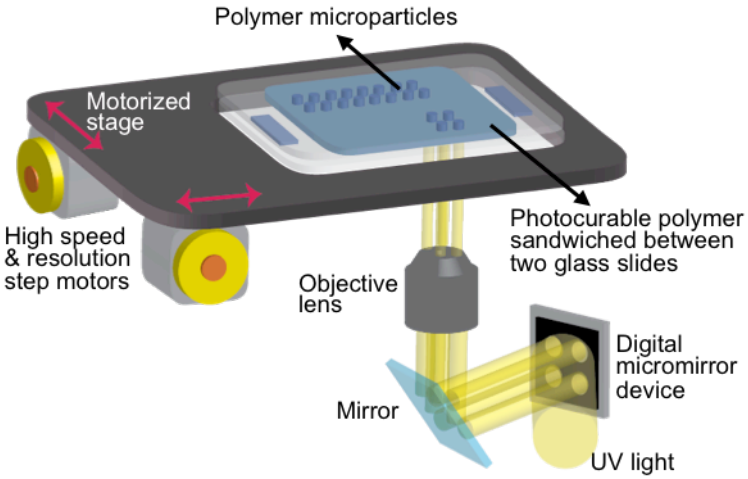

Figure 2.4 Maskless lithography system with a motorized stage and its step-and-repeat operation.

Briefly, the procedure of microparticle fabrication using this step-and-repeat maskless lithography system is as follows. As a substrate for the microparticle fabrication, polydimethylsiloxane (PDMS)-coated glass slides are prepared by spin coating PDMS elastomer (Sylgard 184, Dow Corning) on a glass slide for 30 s at 3,000 r.p.m., followed by thermal curing for 10 min on a 150 °C hot plate. A photocurable polymer solution is dispensed between two PDMS-coated glass slides separated by thin spacers. Microparticles with various shapes are polymerized in a

step-and-repeat manner with patterned UV light reflected by a DMD (Texas Instruments) and projected through an objective lens. After collecting the fabricated microparticles in a conical tube, they are washed in ethanol for 1 hour to remove unpolymerized monomers.

The throughput of microparticle fabrication (T) can be calculated as

$$T = \frac{N_p}{t_{polymerization} + t_{step}} \tag{2.1}$$

where N_p is the number of microparticles fabricated in one exposure, $t_{polymerization}$ is time to polymerize microparticles, and t_{step} is time to move one step. If I fabricate with microparticles with the size of 250 μm using prepolymer solution composed of 90 vol% poly(ethylene glycol) diacrylate (PEGDA, Mn=700) as a polymer resin and 10 vol% 2-hydroxy-2-methyl-1-phenyl-propan-1-one (DAROCUR 1173, BASF Resins) as a photoinitiator, N_p is 4, $t_{polymerization}$ is 0.1 s and t_{step} is 0.032 s when 10x objective lens is used. In this case, the fabrication throughput of microparticle is approximately 30 per a second, which a few hundreds of thousand of particles can be fabricated in a day.

Table 2.1 Specification of the developed maskless lithography system.

Magnification of objective lens	Exposure of UV light (365 nm)		t_{step} (s)
	Area (μm^2)	Energy (mW/cm^2)	
10x	650 × 870	147	0.032
20x	325 × 435	588	0.018

On the basis of this step-and-repeat fabrication of microparticles using maskless lithography, I have developed two types of encoded microparticles and one microchip coating technique for three specific applications: QR-coded microtaggants for anti-counterfeiting of drugs, amphiphilic droplet carriers for multiplexed liquid loading, and conformal phosphor coating technique for light-emitting diodes.

QR-coded Microtaggants for Anti-counterfeiting of Drugs

A microtaggant, which is a microscopic and traceable particle added to materials or products for authentication, is emerging as a superior tool for on-dose authentication (ODA) for anti-counterfeiting of drugs [42]. ODA tags an individual unit-of-dose form at the drug formulation level. The microtaggant is included in an individual tablet or capsule during the drug formulation process and can be used for the authentication and identification of the drug itself. This method is simple and powerful, because the micrometer-scale physical identifiers in the unit-of-dose drug cannot be easily copied and replaced with fake ones. Recently, polymer microbeads and microfibers have been utilized as microtaggants [43-45]. In order to specify certain drug information (e.g. the producer name, lot number, date of production, and expiration date) a conventional graphical code in the form of a one-dimensional (1D) barcode or letters is printed onto the microparticles by the spatial selective photobleaching of the fluorescence. However, the conventional code scheme on the

microtaggant can only provide limited features for drug authentication. The data capacity may be insufficient to support a large amount of drug information, because only short text strings or a simple barcode can be printed on the microtaggant surface. In addition, restoring data from a damaged code is impossible because the simple graphical encoding scheme has no corresponding error correction algorithm.

Quick Response (QR) code is a 2D matrix code that combines a high capacity with error correction features [46-48]. This dot-based, 2D binary code scheme can provide a higher density of binary code information than a line-based 1D barcode scheme, and multilevel coding allows data from a partially damaged code to be recovered. In addition, omnidirectional reading without in-plane directional alignment, which is an advantageous feature for high-speed authentication, is possible on account of its specific patterns. All these features of QR Code can provide a microtaggant with a high-level authentication capability.

I have developed a QR-coded microtaggant that allows the encoding of a large amount of data that will not be lost during the drug formulation process (figure 2.5a). In this work, QR-coded polymeric microtaggants are fabricated by photopolymerization of PEGDA through a single exposure to QR code-patterned UV light. A fluorescence acrylic monomer (methacryloxyethyl thiocarbamoyl rhodamine B) is mixed with the polymer solution to give the QR code pattern a vivid color, making it cleary distinguishable from the background with the use of a

digital detector (figure 2.5b). These microtaggants offer all the unique features of QR Code, such as high-capacity encoding, error correction capability, and omnidirectional reading. I have also demonstrated the complete process of drug authentication using QR-coded microtaggants, from the formulation of the microtaggant-equipped capsule to the decoding step using a QR code reader application on a smartphone (figure 2.5c).

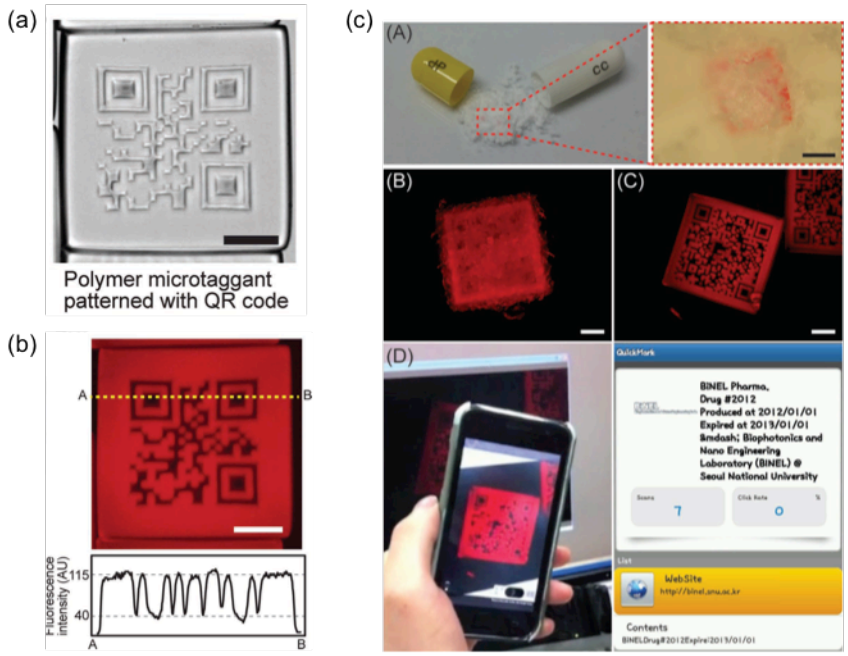

Figure 2.5 QR-coded microtaggants for anti-counterfeiting of drugs: (a) a microscope image of polymer microtaggant patterned with QR code (scale bar: 200 μm); (b) a fluorescence microscope image of the QR-coded microtaggant and the line profile of the fluorescence intensity (scale bar: 100 μm); (c) the authentication process for the anti-counterfeiting of a drug capsule using QR-coded microtaggants (scale bar: 200 μm, 100 μm, 100 μm in order of appearance).

Amphiphilic Droplet Carriers for Multiplexed Liquid Loading

Recently, encoded hydrogel technology has been evolving by adding multi-functional capabilities to particles [49, 50] or developing microfluidic devices for particle-based assays [51, 52]. For example, magnetic barcode hydrogel enables particle manipulation such as separation, alignment[49], and mixing [50] when used in flow through device. These efforts have been building to provide a powerful platform for particle-based multiplex assays, which can provide high-throughput screening capabilities and higher sensitivity with smaller volume along with all the functionality of conventional high-throughput screening technology [53]. However, some challenges still remain in particle-based multiplex technology in their current state.

Liquid handling is generally a challenge in high-throughput multiplex assays. In order to increase the screening throughput, the number of reaction sites increases and reaction volume decreases [54]. However, as reaction volume decreases, conventional liquid handling methods based on pipetting have challenges such as small volume drop evaporation and inaccurate volume dispensing. Microfluidic technology has been providing numerous solutions to overcome these challenges [55]. Recent research on small volume liquid dispensing has focused on microfluidic reactors in a microfluidic device using microcomponents such as microvalves and micropumps [56, 57]. However, little research has been done on precise liquid loading of microstructures in a microfluidic device. Dispensing liquid into hydrogel

microstructures would be applicable to analysis of reaction kinetics or cellbased bioassays in structurally isolated, but movable picoliter volumes.

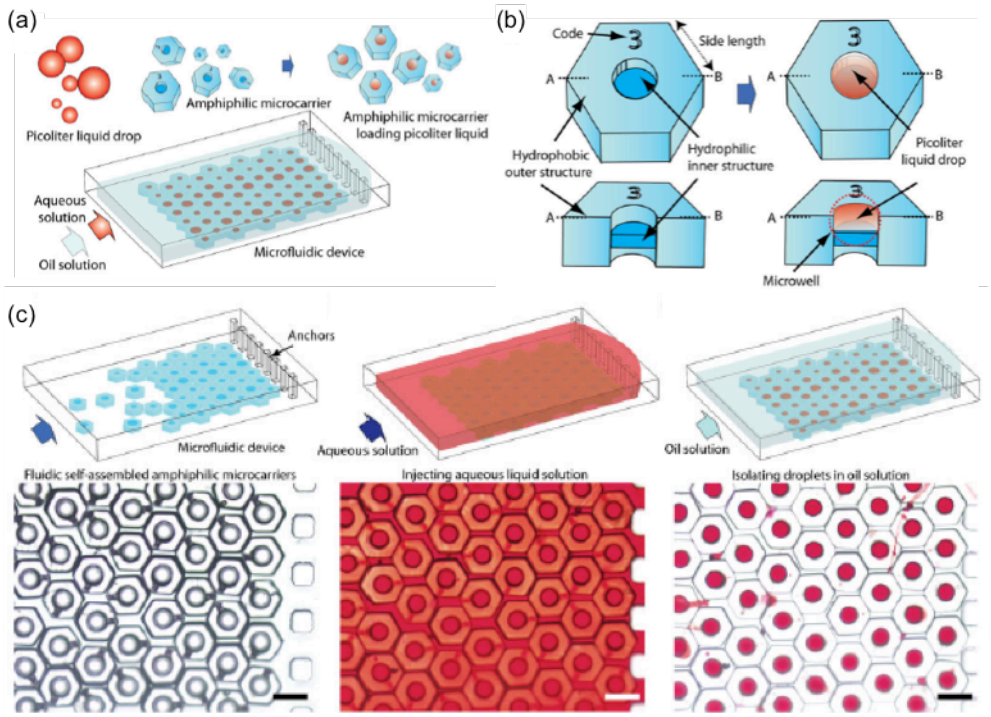

Figure 2.6 Amphiphilic microcarriers for loading picoliter liquid: (a) a schematic diagram of the amphiphilic microcarriers; (b) a structure of amphiphilic microcarriers composed of a hydrophobic outer structure with a graphical code and a hydrophilic inner structure; (c) high-throughput loading of picoliter droplets into free-floating amphiphilic microcarriers (scale bar: 100 μm)

I have developed an encoded amphiphilic microcarrier and a microfluidic system for loading quantized picoliter liquid volumes into amphiphilic droplet microcarriers, composed of hydrophobic hexagonal outer structure and hydrophilic

inner structure (figure 2.6(a, b)). In addition, they have graphical codes on the hydrophobic structure for easy identification. The free-floating carriers are fabricated by serial photopolymerization of hydrophobic trimethylolpropane triacrylate (TMPTA) and PEGDA, and fluidically assembled in a microfluidic channel. With this assembled microdevice, I have demonstrated the simultaneous loading process of multiple picoliter liquid droplets by serial injection of aqueous and oil solutions (figure 2.6(c)).

Conformal Phosphor Coating Technique for Light-emitting Diodes

As traditional light sources are being phased out in backlighting, automobile, and indoor/outdoor lighting markets, the demand for high-quality white LEDs has increased substantially [58]. In order to generate white light, most currently produced commercial white LEDs convert the wavelength of light emitted from a chip using one or more phosphor materials. The optical quality of white light from phosphor-converted white LEDs (pc-WLEDs) is critically determined by setting characteristics of the phosphor layer, such as the geometrical shape and thickness [59]. Owing to variations in the height or surface curvature of the phosphor casting within reflector cup packaging resulting from inconsistent dispersal of phosphor-containing material, conventional dispensing methods suffer from non-uniform color distribution and angular color inhomogeneity.

To supply white LEDs within specified and narrow color ranges, packaged pc-

WLEDs must be sorted and selected by chromaticity. Because this color binning process is carried out after packaging has been completed, it results in waste and increased packaging costs. Therefore, development of a process for phosphor coating at the chip level prior to packaging would be helpful in improving the manufacturing efficiency of white LEDs.

To ensure the angular color homogeneity of pc-WLEDs, conformal phosphor coating methods [60-64] have been developed to achieve a consistent phosphor layer thickness around the radiation surface of the LED chip. However, applying a coating to an LED sidewall from which light is also emitted presents a challenge. Additionally, owing to the lack of patterning ability, coating without the use of contact electrodes in the wire-bonding step is impossible, or at least it involves complex, multi-step processes; thus, coating is only applicable to a flip chip configuration or following wire-bonding packaging.

Recently, automated encapsulation and patterning of randomly dispersed and rotated silicon microchips in microfluidic channels by means of image processing based optofluidic maskless lithography (IP-OFML) [34, 36]. Based on this, I know that a photolithographic approach using image processing based maskless lithography (IP-ML) can be used to conformally phosphor-coat LEDs at a consistent thickness on both the sidewalls and in open-patterns on contacts. In this study, I have developed IP-ML for a conformal, chip-level process that could perform

phosphor coating onto an array of LEDs on a blue tape. In the method, the recognition of individual chips and the generation of corresponding mask images on a spatial light modulator are enabled through the real-time processing of camera images by the IP-ML. This allows accurate control of the conformal phosphor coating, regardless of the positional and rotational displacements of LEDs on the tape originating in the pick-and-place operation of robotic arms (figure 2.7(a)). Figure 2.7(a) also shows a schematic of the conformal phosphor coating process. An LED array is set on a blue tape with inter-chip spacing to allow sidewall coating, and the blue tape is then fastened with a plastic assembly zig. A mixture of yellow phosphor, YAG:Ce, and photo-curable resin (Norland Optical Adhesive 81, NOA81) is then dispensed onto the array. Using spacers and a glass substrate, the thickness of the top coating is set and the top surface of the coating layer is flattened. Prior to this, the glass substrate is coated with polydimethylsiloxane (PDMS) to prevent adhesion between the coating layer and the glass substrate [10]. After the prepared array is located by the IP-ML system, each LED is treated in turn. First, an image of an LED is captured with a bottom-view camera. UV light is reflected from the pattern image on a digital micromirror device (DMD), and the bottom of the chip is then illuminated to allow conformal coating onto the LED. For chips opaque to UV light, the prepared array is turned upside down in order to illuminate the top surface of the chip, and the phosphor concentration is adjusted in order to capture the chip image

with phosphor particles. The thickness of the sidewall coating is controlled by the DMD pattern so that it matched that of the top coating. This process is carried out for each chip in the array in an automatic, step-and-repeat manner using a motorized stage. Finally, uncured parts of the dispensed mixture are removed with gentle acetone washing, and the LEDs are dried. Using this process, I have fabricated white LEDs that has a narrow color distribution and that are practically packaged on their reflecting cups (figure 2.7(b)). The chromaticity of the white LEDs has been controlled by the coating thickness and the phosphor concentration.

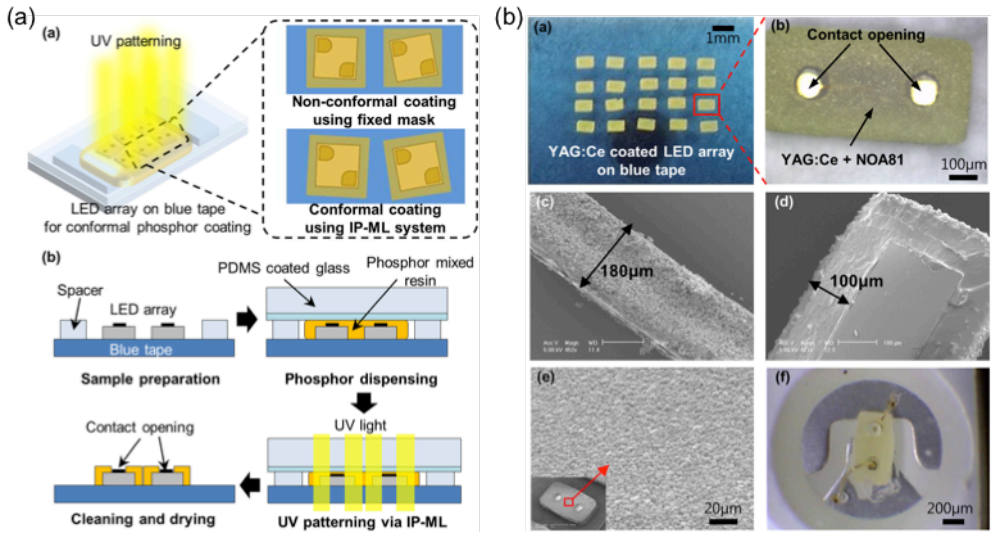

Figure 2.7 Conformal phosphor coating technique using image processing based maskless lithography (IP-ML) for white LEDs: (a) schematic illustration of the technique and sequential procedure; (b) Micrographs of the phosphor-coated LEDs fabricated using IP-ML.

2.2.2 Shape-coded Microparticles for Encoded Viral Micropatch

Microparticles should satisfy at least three requirements to be used for the encoded viral micropatch: 1) their encoding scheme should be compatible with high-content imaging, 2) their surface should be functionalized to immobilize viral vectors, and 3) small molecules can be transported to treat cells under microparticles.

Shape Encoding of Microparticles

Various encoding mechanisms have been proposed to provide a sufficient number of identification codes for microparticles (figure 2.8). Spectroscopic encoding, which relies on both the color and intensity of light emitted from the coloring materials such as fluorescence dyes [65] or quantum dots [66], is the most well-established encoding scheme. The overall spectrum of the coloring materials embedded inside or attached on the surface of microparticles serves as an identification code that can be readout by a spectrometer. However, the possible number of codes is practically limited by the availability of different materials with minimal spectral overlap. More importantly, the spectrum-based detection is severely incompatible with high-content imaging, which uses fluorescent dyes or protein markers to detect the cellular context. On the other hand, graphical encoding is based on the patterning of optically detectable elements on the microparticle surface. Binary barcoding is a popular coding scheme that provides a relatively large encoding capacity [67]. However, its maximum encoding capacity is limited by the particle size. Moreover,

the optical patterns inside microparticles can interrupt optical observation of cells under the microparticles, which is important for detect morphological change or dynamic moving of cells.

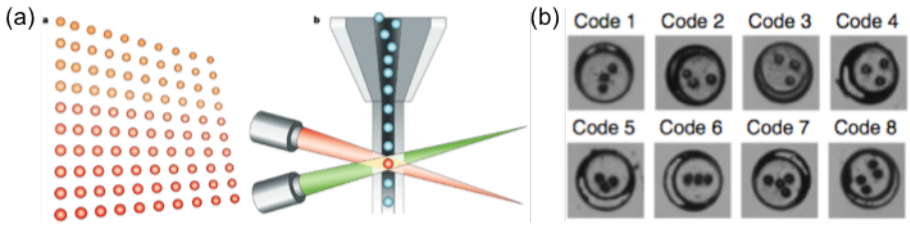

Figure 2.8 Various encoding scheme of microparticles: (a) spectral encoding [68]; (b) barcode-based graphical encoding [69].

Based on these considerations, I decide to use the shape of microparticles as an identification code. In principle, micoparticles can have infinite number of shapes. The shape-based graphical encoding does not restrict high-content imaging including fluorescent and optical observation of cells because an optically recognizable pattern is placed according to the contour of the microparticle. In addition, the shape feature can be easily detectable by machines and human eyes. The shape-coded microparticles can be fabricated using the maskless lithography system described in previous section and controlling patterns on the DMD can support diverse shapes (figure 2.9).

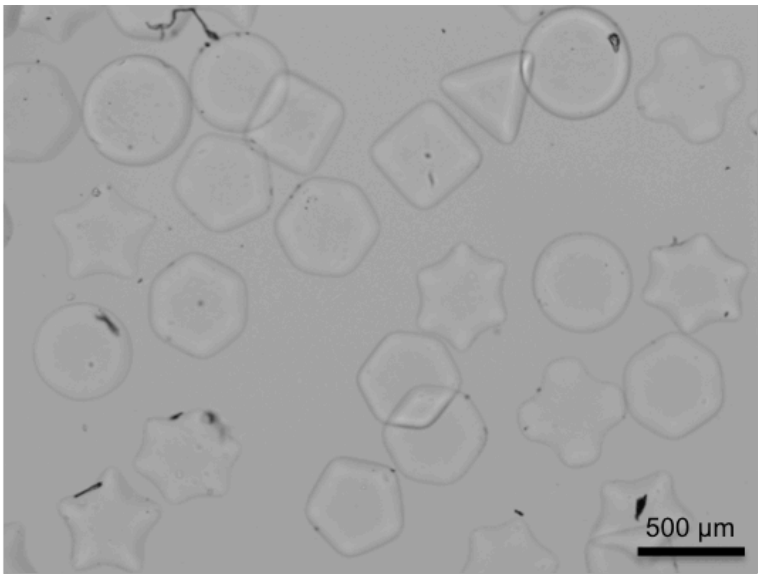

Figure 2.9 Various shape-coded microparticles fabricated using the maskless lithography system.

Chemical Functionalization for Viral Vector Immobilization

In this study, I develop *in situ* functionalization of polymer microparticles. As I mentioned in the introduction section of this chapter, chemically functionalized microparticles can be easily fabricated by just mixing proper materials in photopolymerization process. In this method, I use PEGDA as a photocurable polymer solution since it is known as a non-cytotoxicity material [70] and optically transparent enough to observe cells under the microparticle using an optical microscope. In order to create carboxyl functional groups on the microparticle surface, acrylic acid is incorporated into the PEGDA solution [71, 72]. The amount of acrylic acid in the mixed solution directly controls the amount of surface

functional groups. Figure 2.10 shows the availability of carboxyl groups on the microparticles fabricated using a mixture of PEGDA and acrylic acid with different volume ratios. The particles are reacted with EDC/sulfo-NHS to convert the carboxyl groups to amine-reactive sulfo-NHS esters. The activated particles are then incubated with fluorescein isothiocyanate-conjugated bovine serum albumin (FITC-BSA) for 2 hours at 4 °C in order to examine available carboxyl groups on the surface of microparticles. The particles fabricated using higher volume fractions of acrylic acid had more available carboxyl groups. By considering covalent bonding capability and physical stability of the polymerized microparticles, I decide to use the prepolymer mixture composed of 34 vol% PEGDA and 60% vol% acrylic acid. In addition, 1 vol% of 1-vinyl-2-pyrrolidinone and 5 vol% DAROCUR 1173 are added to the mixture to help photopolymerization.

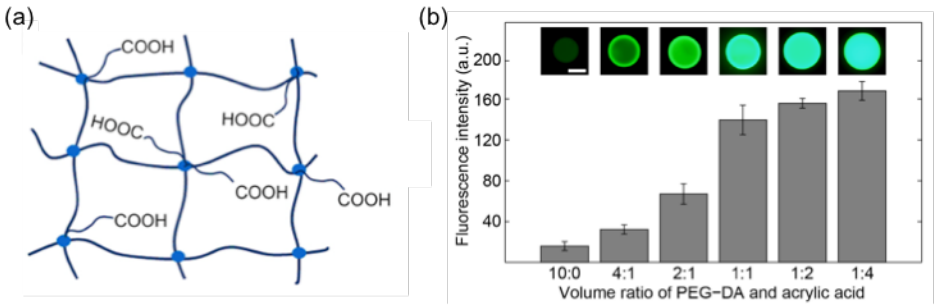

Figure 2.10 Carboxyl functionalization of polymer microparticles: (a) copolymerization of PEGDA and acrylic acid [70]; (b) availability of carboxyl groups on the microparticles according to different volume ratio of PEGDA and acrylic acid examined by FITC-BSA conjugation.

Figure 2.11 shows the suitability of this microparticle for an optical observation of cells and small molecule transportation to cells. The circular microparticles are fabricated with the diameter of 350 μm and the thickness of 80 μm. Cells under the microparticle are clearly seen in visible light illumination through the microparticle. Also, cells under the microparticles are well stained by Hoechst 33342 dye, showing the transportation of small molecules through PEGDA hydrogel porous network in contrast to silica-coated microparticles.

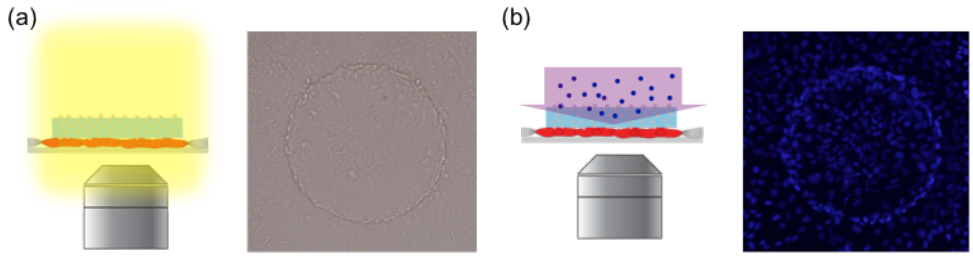

Figure 2.11 Transparency and chemical transportation of PEGDA microparticle: (a) optical observation of cells under the microparticle using a light microscope; (b) Hoechst 33342 staining of cells under the microparticle.

On the basis of investigation in this section, I decide to use in situ carboxyl functionalization method using copolymerization of PEGDA and acrylic acid for the development of the encoded viral micropatch.

2.3 Immobilization of Viral Vectors

2.3.1 Recombinant Adenoviral Vector

Adenovirus (Ad) is well-characterized, non-integrated, non-enveloped, linear double-stranded DNA (dsDNA) virus. Because of its well-known molecular biology, large delivery capacity of foreign DNA fragments, and ability to transduce many cell types, adenoviral vector is widely used for cell-based assays among several viral vectors such as adenovirus, retrovirus and lentivirus-based vectors [73]. Typically Ad2 and Ad5 serotypes are used and these vectors are replication incompetent as the E1 and E3 genes have been deleted. High titer virus preparation can easily be generated using human embryonic kidney 293 (HEK-293) cells [5].

Table 2.2 Properties of viral gene delivery vectors used for cell-based assays

Virus vector	Viral genome	Insert capacity	Vector form	Tropism
Adenovirus (Ad2, Ad5)	dsDNA	8 – 40 kb	Episomal	Broad (cell lines and primary cells)
Lentivirus (HIV-1, SIV)	RNA	8 kb	Integrated	Broad (cell lines and primary cells)
Retrovirus (MLV)	RNA	8 kb	Integrated	Dividing cells only

Structurally, Ads are medium-sized (90–100 nm), non-enveloped viruses with an icosahedral capsid containing a dsDNA genome. Adenoviral capsid, a protein

shell of the adenovirus, consists of 240 hexon proteins and 12 penton bases (figure 2.12). The penton base serves as a hook for the fiber protein that aids in attachment to the host cell via the receptor on the surface of the host cell. Especially, Ads have no viral envelope, a lipid bilayer covering a viral capsid, unlike many other viruses. This feature of Ads is very favorable for specific immobilization on the microparticle because several bio-conjugation methods can be applied using directly exposed capsid proteins.

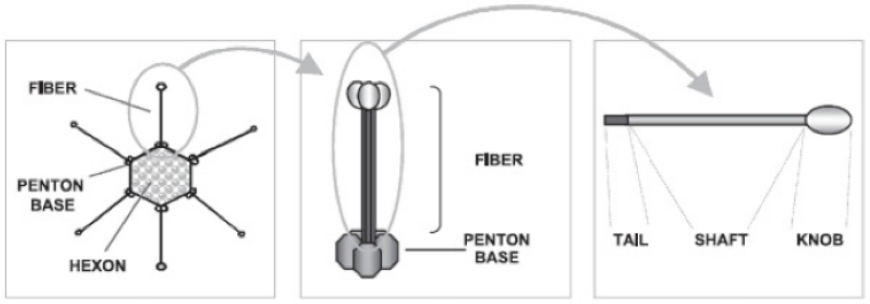

Figure 2.12 Schematic of the adenoviral capsid [73].

Two sequential virus-cell interactions are involved in Ad infection: the primary binding of the viral fiber protein to the cell surface coxsackievirus and adenovirus receptor (CAR), and the secondary interaction of the viral penton base with cell surface $\alpha_v\beta_3$ and $\alpha_v\beta_5$ integrins [74]. The secondary interaction with the integrins is essential for Ad internalization into the cell. Adenoviral capsid proteins dissociate prior to endocytosis, and the decrease of pH value of the viral endosome gives the virus the ability to detach from the vesicle and enter the cytosol. After fragmentation

of capsid proteins, viral DNA crosses via nuclear pores (figure 2.13).

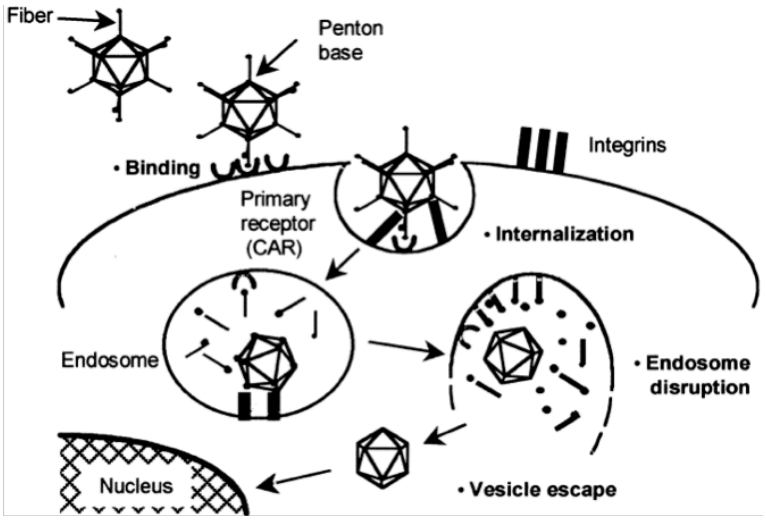

Figure 2.13 Pathway of adenoviral infection [75].

2.3.2 Direct Targeting of Viral Capsid via Carbodiimide Crosslinker (Type 1 Encoded Viral Micropatch)

As described in previous sections, the microparticles have carboxyl groups on the surface and adenoviruses have capsid proteins on the surface, which has primary amine groups. The common method for crosslinking carboxylic acids to primary amines is to use carbodiimide compounds such as EDC. As shown in figure 2.14, EDC reacts with carboxylic acid groups to form an active O-acylisourea intermediate that is easily displaced by nucleophilic attack from primary amino groups. The primary amine forms an amide bond with the original carboxyl group. However, O-acylisourea intermediate is unstable in aqueous solutions, resulting in

decrease of coupling efficiency. Addition of Sulfo-NHS to this EDC-mediated coupling increases efficiency [76].

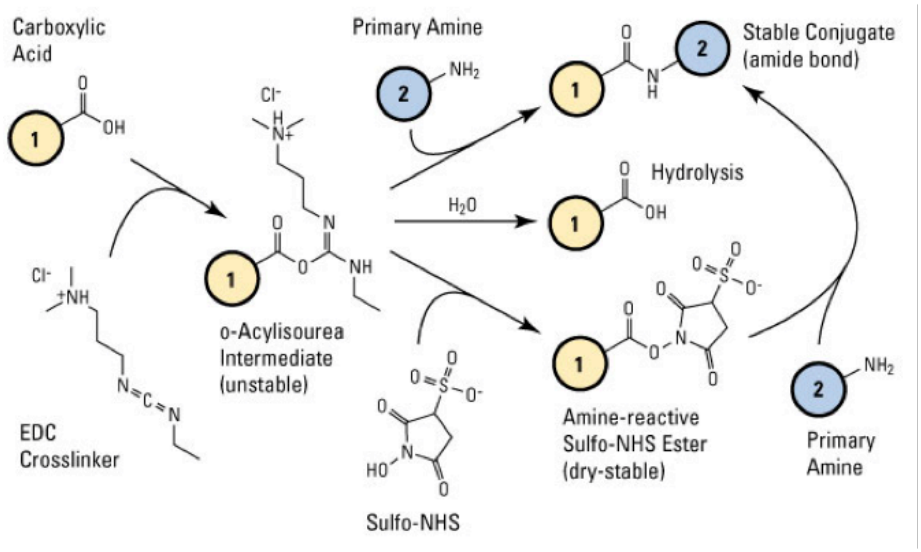

Figure 2.14 EDC plus Sulfo-NHS crosslinking reaction scheme [76].

Materials

Replication-deficient adenoviral vectors expressing green or red fluorescent protein (Ad-GFP and Ad-RFP) are purchased from Vector Biolabs (Philadelphia, PA, USA). All viruses are prepared in phosphate buffered saline (PBS). EDC and Sulfo-NHS are purchased from Sigma-Aldrich and Alfa Aesar, respectively. MES buffer with 0.005% Tween 20 (MEST) is prepared by dissolving MES buffered saline powder (BupH MES Buffered Saline Packs, Thermo Fisher Scientific) in 500 ml of

deionized water with 25 µl of Tween 20 (Sigma-Aldrich). PBS buffer with 0.005% Tween 20 (PBST) is prepared by dissolving phosphate buffered saline powder (BupH Phosphate Buffered Saline Packs, Thermo Fisher Scientific) in 500 ml of deionized water with 25 µl of Tween 20. Anti-adenovirus fluorescein isothiocyanate (FITC)-labeled antibody is purchased from Millipore (Cat. No. 5016).

Immobilization of Adenoviral Vectors

The application of this method for development of the encoded viral micropatch is illustrated in figure 2.15. Firstly, the fabricated microparticles are washed 3 times in MEST. Then, approximately 600 microparticles are treated with a solution of 2 mg of EDC, 4 mg of Sulfo-NHS, and 400 µL of MEST for 30 min at room temperature. The reacted microparticles are washed 2 times with PBST. The microparticles and 10^8 PFU of adenoviral vectors are incubated together overnight at 4 °C with a gentle vortexing. PFU means a plaque-forming unit, which represents the number of infectious viruses. Finally, the microparticles are washed 4 times with PBST to remove unbound adenoviral vectors.

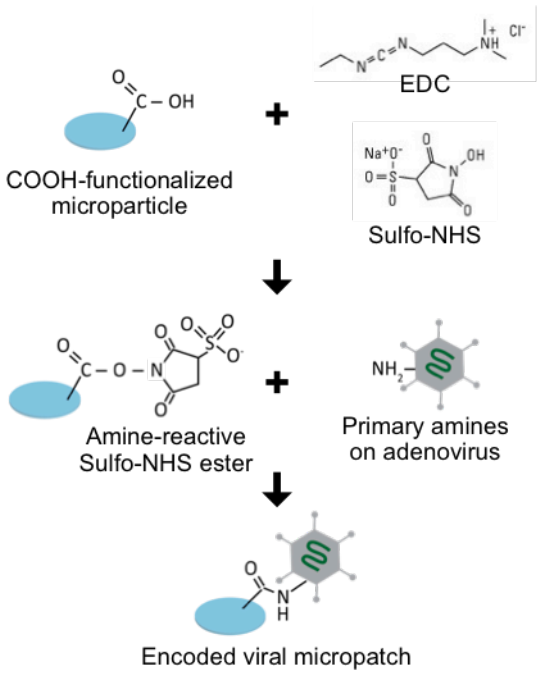

Figure 2.15 Schematic illustration of adenoviral vector immobilization on the microparticle via EDC/Sulfo-NHS method.

The immobilization of adenoviral vectors on the microparticles is confirmed by immunofluorescence test and scanning electron microscope (SEM) observation. For the immunofluorescence test, I use anti-adenovirus FITC-labeled antibody, targeting the hexon protein of adenovirus capsid. The fabricated encoded viral micropatches are incubated with the 1/200 diluted antibody solution for 1 hour. After washing 5 times with PBS, the viral micropatch is observed using a confocal laser scanning microscope. Green fluorescence signal from FITC-labeled anti-adenovirus antibody capturing the immobilized adenoviral vector are well observed (figure 2.16).

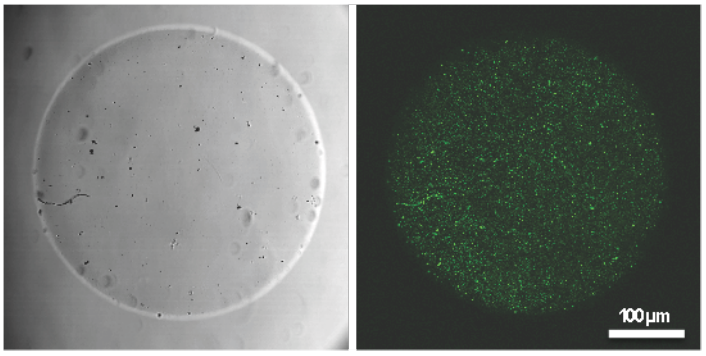

Figure 2.16 Detection of the immobilized adenoviral vectors on the microparticle using FITC-labeled adenovirus antibody.

For the SEM observation, the encoded viral micropatches are fixed in PBS containing 1.5% glutaraldehyde for 5 min at room temperature, followed by 1 hour of incubation in 1% osmium tetroxide (OsO_4) / PBS at room temperature [77]. After washing with deionized water, the samples are dried and coated with platinum (Pt) for SEM observation. As shown in figure 2.17, the immobilized adenoviral vectors are identified based on their typical size (90–100 nm) and icosahedral shape.

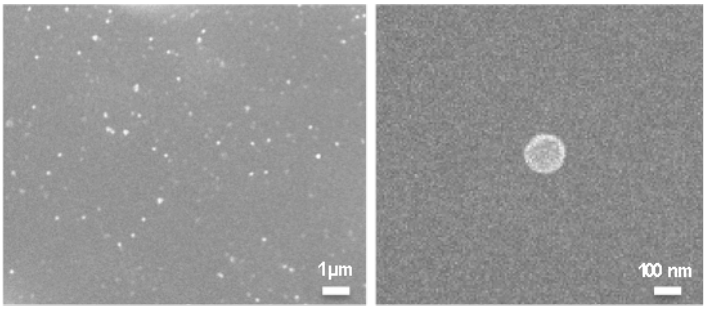

Figure 2.17 SEM observation of the immobilized adenoviral vectors on the microparticle using EDC/Sulfo-NHS.

2.3.3 Indirect Targeting of Biotin-tethered Viral Capsid via Avidin (Type 2 Encoded Viral Micropatch)

The second strategy for the adenoviral vector immobilization is to utilize biotin-avidin binding. Avidin is a protein that shows considerable affinity for biotin. It has the ability to bind up to four biotin molecules (figure 2.18). The avidin-biotin complex is the strongest known non-covalent interaction between a protein and ligand. The bond formation between them is rapid, and once formed, is unaffected by extremes of pH, temperature, organic solvents and other denaturing agents. These features are useful for immobilizing adenoviral vectors through conjugation of capsid proteins to either component of the interaction [78].

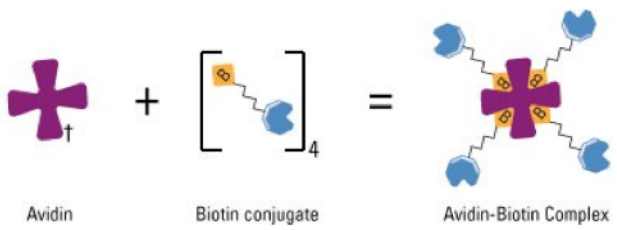

Figure 2.18 Schematic of the avidin-biotin interaction [78].

The application of this interaction for development of the encoded viral micropatch is illustrated in figure 2.19. In this method, I biotinylate both the microparticles and the adenoviral vectors and use avidin-mediated combination to link them [77]. The shape-coded microparticles and adenoviral vectors are biotinylated by conjugating an amine-activated biotin reagent to the carboxyl groups

on the particle and an amine-reactive biotin reagent to the primary amines on the viral capsid. Finally, these two biotinylated materials were combined by reaction with avidin.

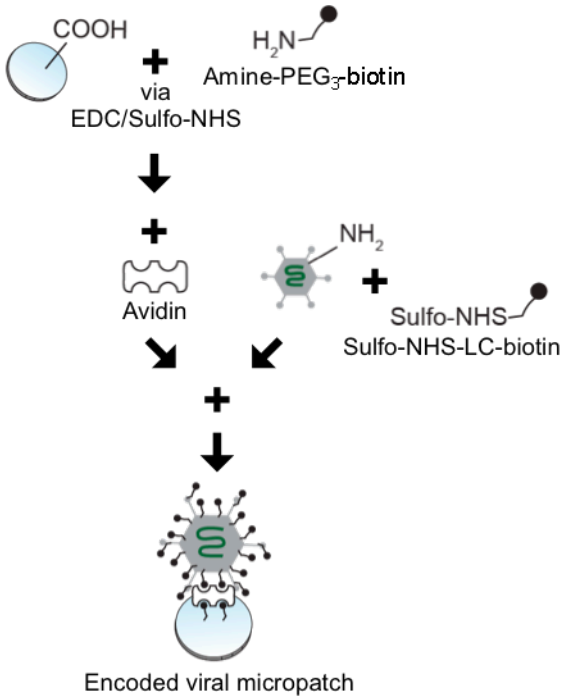

Figure 2.19 Schematic illustration of adenoviral vector immobilization on the microparticle using avidin-biotin interaction.

Materials

Biotinylation reagents (EZ-Link Amine-PEG_3-Biotin, Sulfo-NHS-LC-Biotin, and Biotin-Fluorescein) and fluorescein-conjugated avidin are purchased from Thermo Fisher Scientific Inc. (Rockford, IL, USA). Avidin is purchased from Sigma-Aldrich.

One M glycine solution is prepared by dissoving 75.07 mg in 1 ml of PBS solution.

Biotinylation of Microparticles and Adenoviral Vectors

In order to figure out the proper amount of amine-activated biotin (amine-PEG_3-biotin) to maximize avidin conjugation, the microparticles are biotinylated with different amount of the biotin reagent and examined using FITC-conjugated avidin. The microparticles with the carboxyl functional groups are washed 3 times in MEST. Approximately 600 microparticles are treated with a solution of 2 mg of EDC, 4 mg of Sulfo-NHS, and 400 μL of MEST for 30 min at room temperature. After washing with PBST, the microparticles are biotinylated by reacting with amine-PEG_3-biotin in 200 μL of PBST for 2 h at room termperature. Five different amount of the biotin reagent (0, 10, 50, 100 and 500 μg) are used for the microparticle biotinylation. To conjugate FITC-avidin on the biotinlyated surface of the microparticles, the microparticles are washed 2 times with PBST and then, vortexed gently in 200 μl of PBS solution containing 1% BSA for 2 hours at room temperature to block non-specific absorption of FITC-avidin. After 2-time washing with PBST, the biotinylated microparticles are incubated with 0.02 μg of FITC-avidin in 200 μl of PBST for 2 hours at room temperature. To observe the microparticles on a fluorescence microscope, the microparticles are washed 2 times with PBST.

Figure 2.20 shows the fluorescence micrographs of the biotinylated microparticles after the reaction with FITC-conjugated avidin and the graph of

average fluorescence intensities of the microparticles in each condition. The avidin binding on the biotinylated microparticle surface is maximized when 50 μg of amine-PEG_3-biotin is used for 600 microparticles.

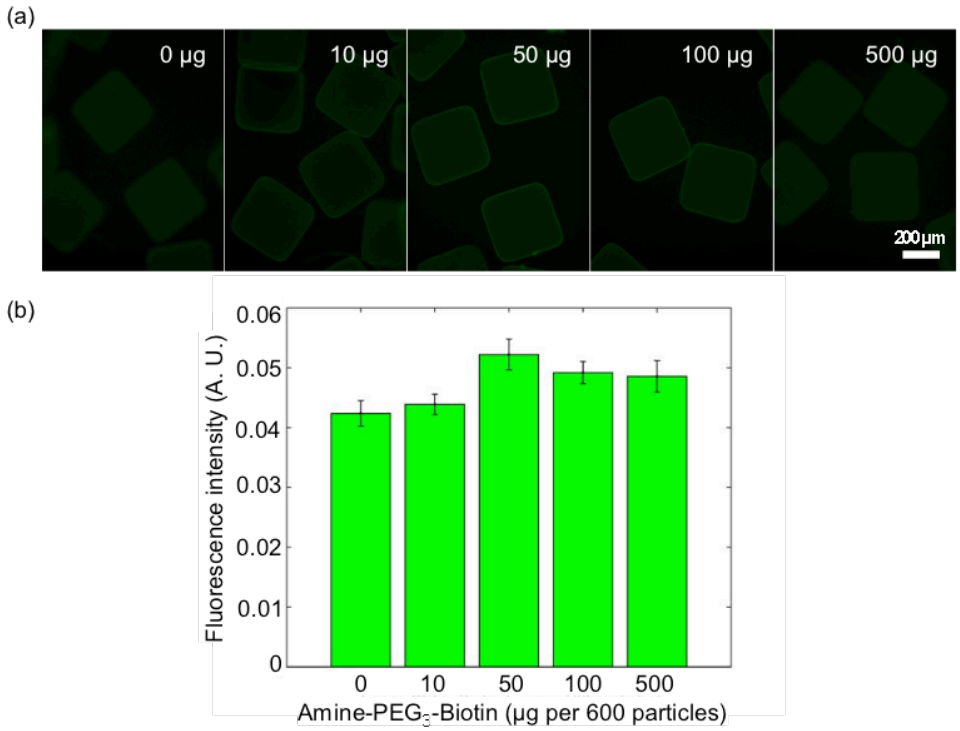

Figure 2.20 An examination of the microparticle biotinylation using FITC-conjugated avidin: (a) fluorescence micrographs of the microparticles biotinylated with amine-PEG3-biotin and probed with FITC-conjugated avidin; (b) Average fluorescence intensities of the microparticles.

The biotinylation of adenoviral vectors are performed using an amine-reactive biotinylation reagent. Adenoviral vectors (10^8 PFU) are incubated in 400 μl of

Sulfo-NHS-LC-biotin dissolved in PBS (5 mg/ml) for 2 h at 4 °C. Quenching unreacted biotin reagent is performed by adding 200 μL of 1 M glycine solution. After 0.5 h of incubation at 4 °C, ultrafiltration is done using an Amicon Ultra-4 centrifugal filter (50 kDa MWCO, EMD Millipore, Billerica, MA, USA) to remove unreacted biotin.

Avidinylation of the Biotinylated Microparticles

In order to figure out the proper amount of avidin for maximizing binding of the biotinylated adenoviral vectors, the biotinylated microparticles are avidinylated with different amount of avidin and the effective biotin binding sites on the avidinylated microparticles are examined using fluorescein-conjugated biotin. Based on the result in previous section, the microparticles functionalized with the carboxyl groups are fabricated and then biotinylated using 50 μg of amine-PEG_3-biotin for approximately 600 microparticles to maximize the biotinylation of the microparticles. After washing 2 times with PBST, the biotinylated microparticles are incubated with avidin in 200 μl of PBST for 2 hours at room temperature. Ten different amount of the avdin (0, 1, 2.5, 5, 7.5, 10, 25, 50, 75 and 100 μg) are used for the avidin conjugation on the biotinylated microparticles. To conjugate fluorescein-conjugated biotin on the avidinylated surface of the microparticles, the microparticles are washed 2 times with PBST and then, vortexed gently in 200 μl of PBS solution containing 1% BSA for 2 hours at room temperature to block non-

specific absorption of fluorescein-conjugated biotin. After 2-time washing with PBST, the avidinylated microparticles are incubated with 200 µl of 0.3 µg/ml fluorescein-conjugated biotin solution for 2 hours at room temperature. Finally, the microparticles are washed 2 times with PBST.

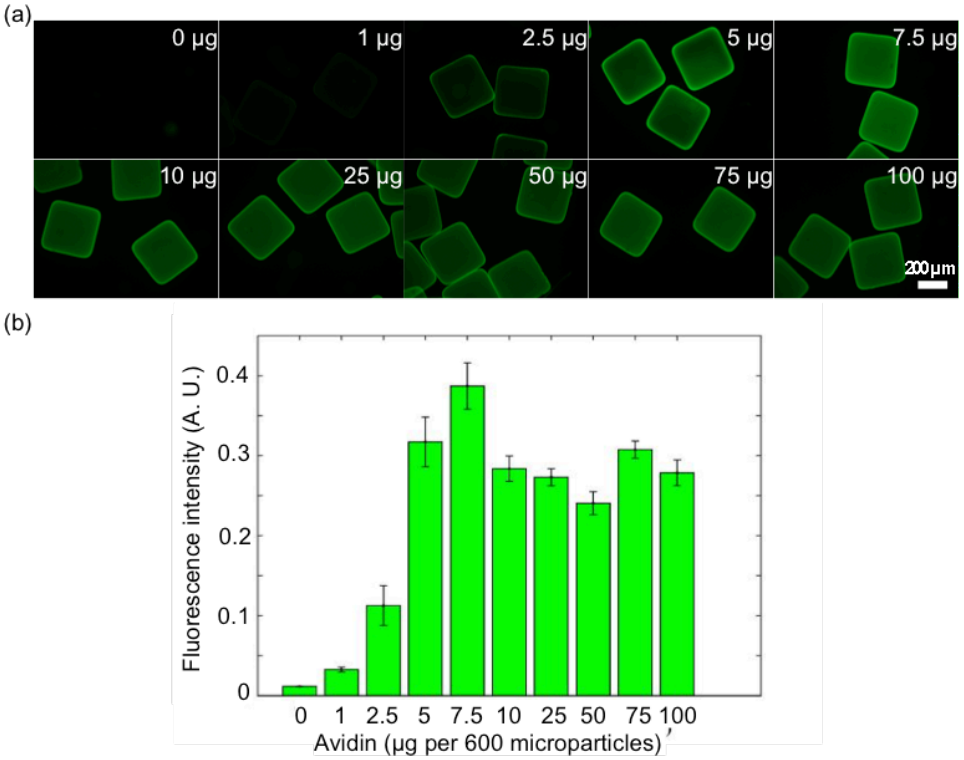

Figure 2.21 An examination of the micropartice avidinylation using fluorescein-conjugated biotin: (a) fluorescence micrographs of the microparticles avdinylated and probed with fluorescein-conjugated biotin; (b) Average fluorescence intensities of the microparticles.

Figure 2.21 shows the fluorescence micrographs of the avidinylated microparticles after the reaction with fluorescein-conjugated biotin and the graph of average fluorescence intensities of the microparticles in each condition. The effective biotin binding sites is maximized when avidin is used 7.5 μg for 600 microparticles.

Immobilization of Biotinylated Adenoviral Vectors

The microparticles are prepared on the basis of the results in previous sections. In detail, The microparticles functionalized with the carboxyl groups are washed 3 times in MEST. Approximately 600 microparticles are treated with a solution of 2 mg of EDC, 4 mg of Sulfo-NHS, and 400 μL of MEST for 30 min at room temperature. After washing with PBST, the microparticles are biotinylated by reacting with 50 μg of amine-PEG_3-biotin in 200 μL of PBST for 2 h at room temperature. The biotinylated microparticles are washed with PBST 2 times and then incubated with 7.5 μg of avidin in 200 μL of PBST for 2 hours at room temperature. The avidin-conjugated particles are then washed with PBST 2 times to remove unbound avidin molecules.

For the immobilization of the adenoviral vectors on the microparticles, the avidin-conjugated microparticles and the biotinylated adenoviral vectors are gently vortexed together in 400 μL of PBST for 2 h at 4 °C. Finally, the microparticles are washed with PBST 5 times to remove unbound viral vectors.

The immobilization of adenoviral vectors on the microparticles is confirmed by SEM observation. For the SEM observation, the encoded viral micropatches are fixed using glutaraldehyde and OsO_4 as described in previous section. As shown in figure 2.22, the immobilized adenoviral vectors are identified based on their typical size (90–100 nm) and icosahedral shape. In addition, unlike the case of EDC/Sulfo-NHS method, biotin molecules are observed on both surfaces of the microparticle and the adenoviral vectors.

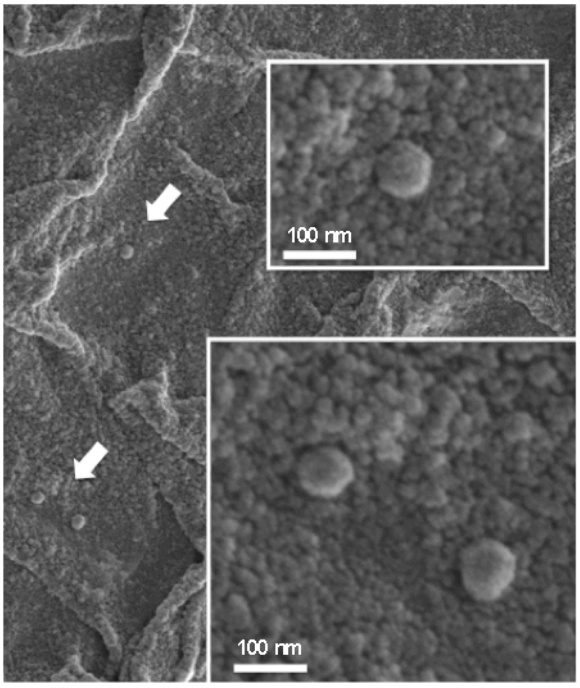

Figure 2.22 SEM observation of the immobilized adenoviral vectors on the microparticle using avidin-biotin interaction.

2.4 Conclusion

In chapter 2, I developed the encoded viral micropatch including the fabrication of shape-coded microparticles and the immobilization of adenoviral vectors on the microparticles. The fabrication of encoded microparticles with various shapes was achieved by developing maskless lithography system supporting an automated step-and-repeat operation. The surfaces of the microparticles were *in situ* functionalized to have carboxyl groups when they were photopolymerized by adding acrylic acid to photocurable resin. Based on this functionalization, two strategies for adenoviral vector immobilization were developed. The first approach was to directly link carboxyl groups on the microparticle and primary amine groups on adenoviral capsid via EDC/Sulfo-NHS. The other approach was to biotinylate both the microparticles and the adenoviral vectors and use avidin-mediated combination to link them. The immobilization of adenoviral vectors on the microparticles in both approaches was confirmed by immunofluorescence test or SEM observation.

Chapter 3

Localized Viral Gene Delivery

In this chapter, I evaluate the localized gene delivery of the encoded viral micropatches developed in previous chapter. The encoded viral micropatches are fabricated with adenoviral vectors carrying fluorescence protein genes and the expression of fluorescence proteins in cells under and outside the micropatch is quantitatively analyzed to rate the localized gene delivery. Also, the principles and characteristics of the localized gene delivery are discussed.

3.1 Introduction

As introduced in chapter 1, cell microarray technologies have been developed to allow perturbing a large number of gene products in a fast way. To date, planar microarrays using robotic spotting of viral solutions on a glass slide [20-23] and a suspension microarray using electrostatic immobilisation of viral vectors on encoded microspheres [28] have been developed for the multiplex cell-based assays based on the reverse transduction. These platforms enable cell-based assays to be conducted in high-density format over standard multi-well plates for high-throughput screening. However, in contrast to multi-well plates, the microscope slide-based cell microarrays are susceptible to contamination among neighboring spots, which hinders accurate quantification in cell-based screening assays [79]. Also, the encoded microsphere-based suffers from the difficulty of optimal cell growth on the microspheres [28].

There are two main reasons of contamination of genetic content present in different spots: transduction at early times after cell seeding and cell migration. Cells uptake genetic material on one spot before they stably attach and then tend to migrate away from the features on which they originally land and intermix with cells on neighboring features [23, 79]. Adding a washing step after cell seeding, increasing the spot-to-spot distance, and blocking cell adhesion outside the spots can reduce the cross-contamination between the spots. However, it is known that this

phenomenon depends on specific adhesion and migration properties as well as transfection ability of different cell lines, these additional efforts need to be optimized according to cell types. Furthermore, increasing the spot-to-spot distance reduces the spatial density of printed features and thus a low number of samples can be studied. Thus, a universal method that accomplishes highly localized gene delivery with a low rate of contamination is required regardless of cell types.

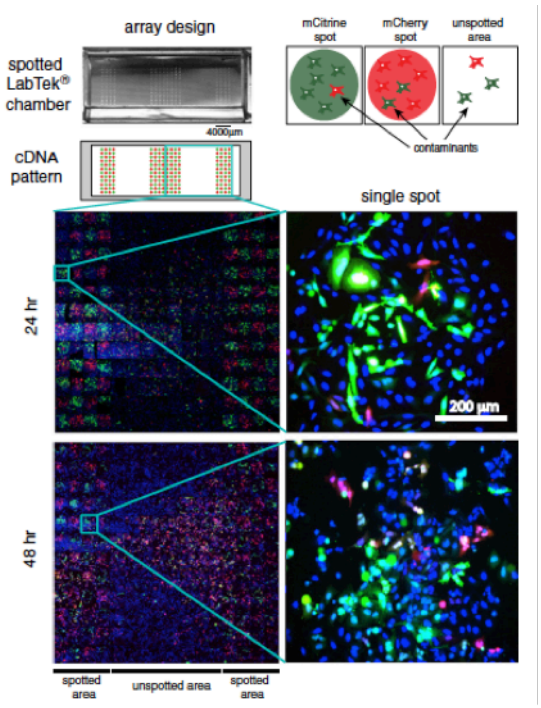

Figure 3.1 Interspot contamination in cell microarray [79].

In the case of cell microarray using the encoded microsphere, agitation cell culture is needed to ensure an optimal cell growth and separation of microspheres

bearing different types of viral vectors [28]. The precipitation of the microspheres prevents an optimal cell growth and allows cells to move across the connected microspheres. Thus, for accomplishing the localized viral gene delivery to cells on the microspheres, a culture condition with a gentle agitation should be established. However, because the agitation culture is unusual in normal cell cultures, it is favorable to develop localized gene delivery methods using encoded microparticles in a suitable form for normal cell cultures.

One significant advantage of the encoded viral micropatch is that the localized gene delivery can be achieved by a single pipetting without careful consideration of distances between the micropatches on a cell layer cultured normally without selective blocking of cell adhesion or agitation culture for cell isolation. In this section, I evaluate the localization of adenoviral gene delivery with two types of the encoded viral micropatch developed in chapter 2.

3.2 Localized Gene Delivery with Type 1 Encoded Viral Micropatch

In order to evaluate the localized viral gene delivery with the type 1 encoded viral micropatch fabricated using EDC/Sulfo-NHS method, U-2 OS is cultured using McCoy's 5A medium at 37 °C in 5% CO_2. This medium is supplemented with 10% foetal bovine serum and 1% penicillin-streptomycin. For the transduction, U-2 OS cells are seeded at a density of 8,000 cells per a well in an optically clear-bottomed 96-well plate and incubated overnight in a CO_2 chamber. Adenoviral vector carrying the GFP gene (Ad-GFP)-immobilized on a circular micropatches are then added to the well in which cells are grown with a single pipetting. After a 40-hour incubation, GFP expression in cells is observed using a fluorescence microscope to inspect the transduction of cells (figure 3.2).

Since adenovirus should be internalized into cells for infection as explained in chapter 2, it is predicted to be hard to transduce cells with the immobilized adenoviral vectors on the microparticle utilizing covalent bonding. However, cells under the micropatches are well transduced with the encoded viral micropatch as shown in figure 3.2(b). This result could be explained by the fact that the fiber proteins dissociated from the adenoviral capsid at an early stage of endocytosis [80]. Since the fiber proteins are relatively long compared to adenoviral particle, most of adenoviral vectors might be immobilized on the microparticle through fiber proteins

instead of hexon proteins. Thus, the dissociation of the fiber proteins can allow the separation of the immobilized adenoviral vectors from the microparticle and the internalization of them.

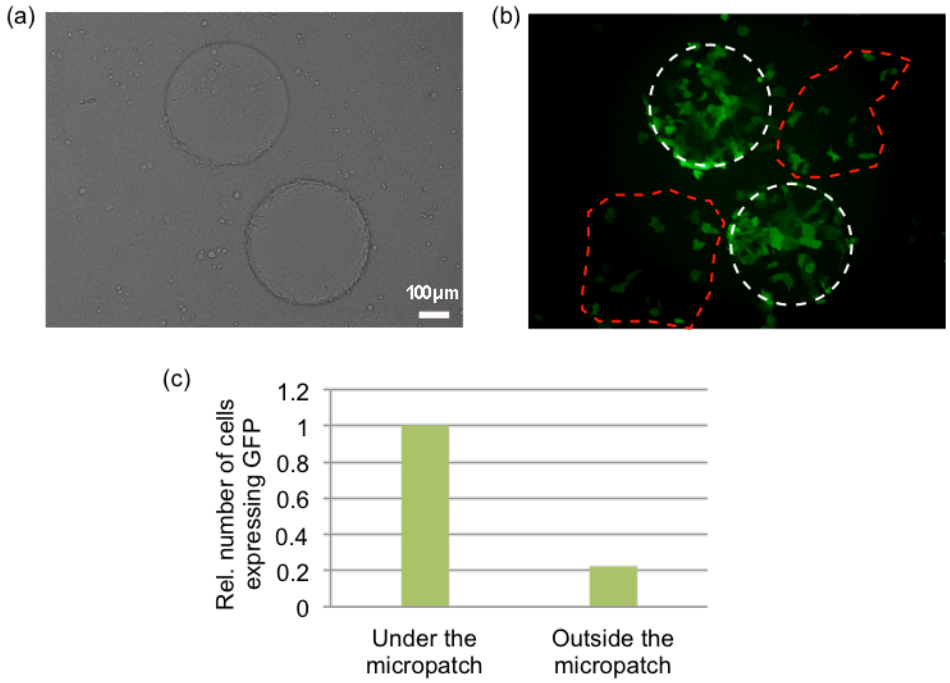

Figure 3.2 Localized gene delivery with the type 1 encoded viral micropatch fabricated via EDC/Sulfo-NHS method: (a) an optical microscope image of the circular-shaped Ad-GFP micropatch on U-2 OS cells; (b) a fluorescence microscope image of GFP expression in U-2 OS cells. White and red dashed lines indicate GFP expression in cells under the micropatches and outside the micropatches, respectively; (c) quantitative evaluation of the number of cells expressing GFP under and outside the micropatches in (b).

However, although most of cells expressing GFP are located under the

micropatch, a considerable number of cells outside the micropatch express GFP. The relative number of cells expressing GFP under and outside the micropatches in figure 3.2(b) is quantitatively measured by calculating green-occupied area in each region. As depicted in figure 3.2(c), the relative number of cells expressing GFP outside the micropatches is approximately 0.2 compared to that under the micropatches. The transduction of cells near the micropatches could result from the local spreading of non-specifically bound adenoviral vectors on the micropatch. Even though the micropatches are thoroughly washed to remove unbound adenoviral vectors at the fabrication step, there is high possibility that non-specifically bound adenoviral vectors still remain. Since this can cause a high rate of contamination of adenoviral gene delivery when heterogeneous types of micropatches are delivered to cells at the same time, the type 1 encoded viral micropatch fabricated via EDC/Sulfo-NHS method is not suitable for achieving highly localized gene delivery.

3.3 Localized Gene Delivery with Type 2 Encoded Viral Micropatch

3.3.1 Evaluation of the Localized Gene Delivery

In order to evaluate the localized viral gene delivery with the type 2 encoded viral micropatch fabricated using avidin-biotin method, U-2 OS cells are prepared in a 96-well plate like in previous section. Figure 3.3 shows localized adenoviral gene delivery to a cell monolayer using the circular Ad-GFP micropatch. After a 2-day incubation, adenoviral transduction is identified by expression of GFP in cells. As shown in figure 3.3(b), GFPs are expressed only in cells under the micropatches and thus, perfectly localized gene delivery is achieved in this trial.

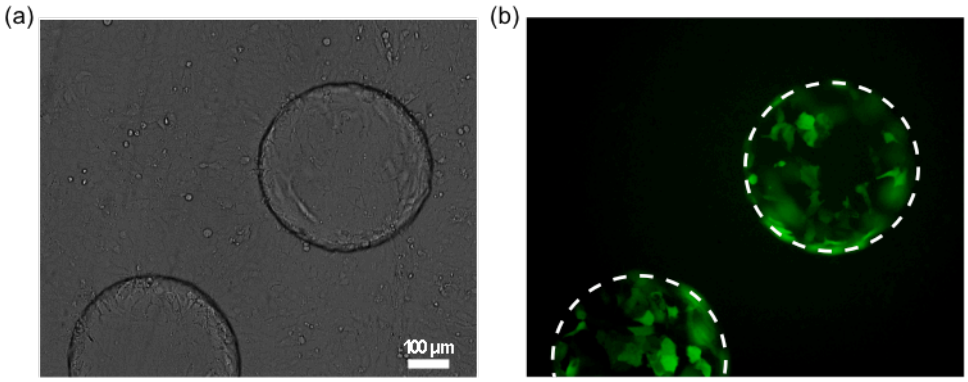

Figure 3.3 Localized gene delivery with the type 2 encoded viral micropatch fabricated via avidin-biotin method: (a) an optical microscope image of the circular-shaped Ad-GFP micropatches on a U-2 OS cell layer; (b) a fluorescence microscope image of GFP expression in U-2 OS cells. White dashed lines indicate outlines of the micropatches.

Based on this encouraging result, multiplexed gene delivery is carried out using two types of encoded viral micropatches: Ad-GFP-immobilized on a circular micropatch and an adenoviral vector carrying the RFP gene (Ad-RFP)-immobilized on a square micropatch in order to measure the cross-contamination. These micropatches are randomly placed on U-2 OS cells grown in a well of a 96-well plate by pipetting them as a mixture. After a 2-day incubation, multiplexed transduction is identified by expression of each fluorescent protein in cells under each micropatch (figure 3.4(a)). Whole area of the well is scanned using a confocal laser scanning microscope and the images of green, red, and transmitted channels are acquired to calculate the number of cells expressing each fluorescence protein. In order to quantitatively measure the cross-contamination between two types of micropatches, the number of cells expressing each fluorescence protein is counted through image processing. The relative number of GFP-expressing cells under the square micropatches is calculated with respect to the number of GFP-expressing cells under the circular micropatches, which is set to 1, and vice versa. Quantification of fluorescent protein-expressing cells under the circular and square micropatches demonstrates no significant cross-transduction (figure 3.4(b)). This result suggests that the type 2 encoded viral micropatch fabricated utilizing avidin-biotin interaction is amenable to multiplex gene delivery for high-throughput cell-based assays.

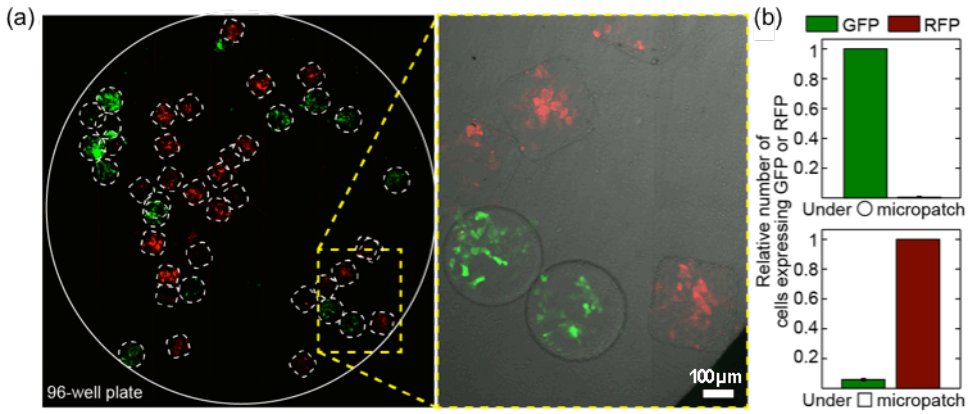

Figure 3.4 Multiplexed gene delivery using circular Ad-GFP and square Ad-RFP micropatches: (a) Overlaid (left: green and red channels, right: green, red, and transmitted channels) and tiled confocal laser scanning microscope images of a well in a 96-well plate, in which the two types of micropatches are simultaneously pipetted; (b) Quantitative analysis of the localized gene delivery in (a). The data represent the mean ± standard deviation of three experiments.

The multiplex gene delivery is also achieved using the encoded viral micropatch and free Ads together. In this case, the free Ad-GFPs are introduced before the encoded viral micropatch with the purpose of co-transducing cells under the micropatch. Free Ad-GFPs are introduced to a well in which U-2 OS cell are grown and the well-plate is incubated for 4 hours to transduce whole cells in the well. Then, square Ad-RFP micropatch are pipetted into the well for the localized co-transduction of Ad-GFP and Ad-RFP. The plate is incubated again for 40 hours for the expression of GFP and RFP in the transduced cells. Figure 3.5 shows the bright-field, green fluorescence, red fluorescence, and overlaid images of green and red fluorescences. Because of highly localized RFP gene delivery with the encoded

viral micropatch, co-transduction indicated by yellow color occurs only under the micropatch as shown in figure 3.5(d). Thus, heterogeneous cell configuration with different protein expressions is achieved in a single well.

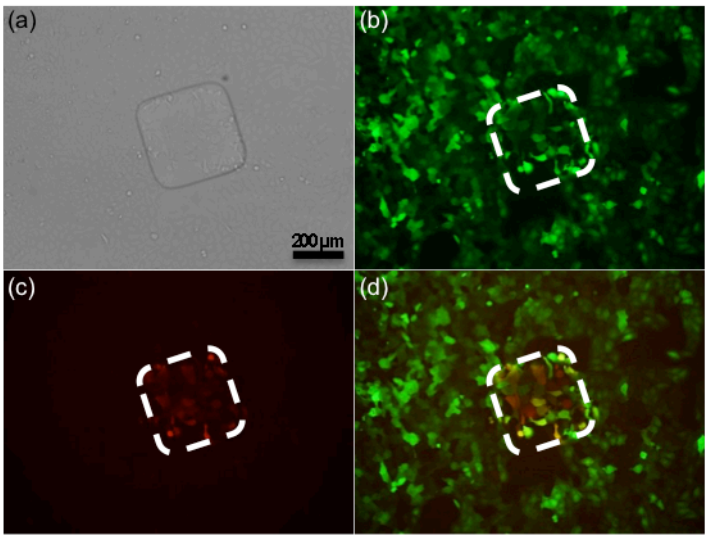

Figure 3.5 Multiplex gene delivery utilizing co-transdcution with free Ad-GFP and Ad-RFP micropatch indicated by white dashed lines: (a) a bright-field image of the micropatched cells; (b) green fluorescence micrograph showing GFP expression; (c) red fluorescence micrograph showing RFP expression; (d) overlaid image of green and red fluorescences.

The number of transduced cells in the localized gene delivery using the encoded viral micropatch can be controlled by adjusting the area covered by the micropatch and the amount of adenoviral vectors used in the immobilization step. I fabricate three different sizes of circular micropathes with Ad-GFP to control the number of transduced cells. The radius of each micropatch is 125, 180, and 280 μm,

thus having 0.48:1.00:2.42 ratio of area covered by a micropatch (figure 3.6(a)). By image processing of green channel images showing GFP expression, it is shown that the number of transduced cells is proportional to the area covered by the micropatch.

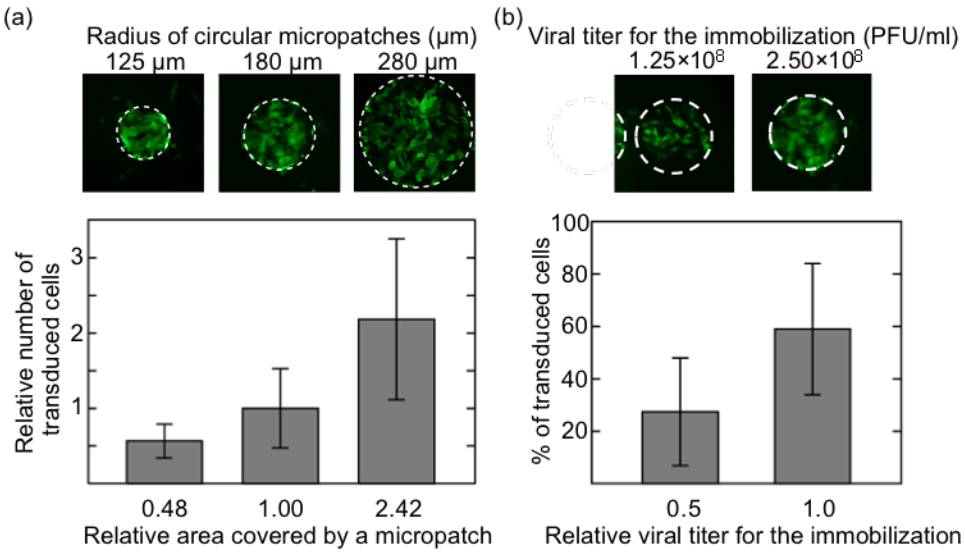

Figure 3.6 Controlling the number of transduced cells under the micropatch: (a) transduction of U-2 OS cells with different size of circular Ad-GFP micropatches. The graph shows the mean values ± standard deviation (total n = 118); (b) transduction of U-2 OS cells with circular Ad-GFP micropatches using different amounts of vectors in the immobilization step. The graph shows the mean values ± standard deviation (total n = 198).

Also, the number of transduced cells is proportional to the amount of adenoviral vectors used in the immobilization step. Two types of circular Ad-GFP micropatches are fabricated using 1.25×10^8 and 2.50×10^8 PFU/ml in the adenoviral vector immobilization step as expecting the linear extent of the immobilization. The

percentage of transduced cells under each type of micropatch shown in figure 3.6(b) says that the adenoviral titer used for the immobilization can control the number of transduced cells. Thus, the localized gene delivery process using the encoded viral micropatch can be controlled for use in various cell-based assays.

3.3.2 Consideration of the Localized Gene Delivery

The strict confinement of adenoviral gene delivery under the micropatches fabricated utilizing avidin-biotin interaction is due to the biotinylation of adenoviruses, which is also used for their immobilization on the microparticles. Cell infection by adenovirus is mainly dependent on the binding of viral fiber protein to an adenoviral receptor, CAR, on the cell surface [81]. The biotinylation of adenovirus shields the fiber protein from primary binding, causing a significant loss of infectivity in the free form. The transduction efficiencies of the biotinylated adenoviral vectors are investigated (figure 3.7). Ad-GFPs are biotinylated with five different concentrations of the biotin reagent, and the biotinylated vectors with different multiplicity of infections (MOIs, the ratio of the number of infectious adenoviral vectors to the number of cells) are used to transduce U-2 OS cells. The transduction efficiencies are calculated by counting GFP-positive cells versus total cells determined by Hoechst 33342 staining. The transduction efficiency decreases as the extent of the biotinylation increases. For the encoded viral micropatch, adenoviral vectors are biotinylated using 5 mg/ml of sulfo-NHS-LC-biotin.

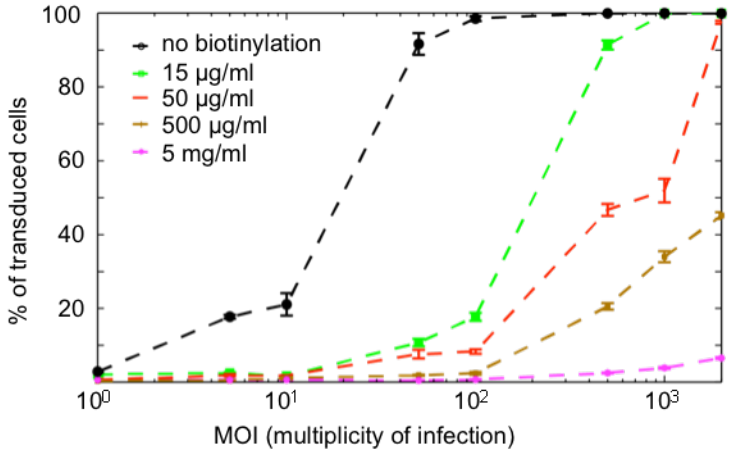

Figure 3.7 Infectivity of biotinylated adenoviral vectors. The error bars represent the standard deviation of the mean from 4 microscopic views for each data point.

However, when the biotinylated adenoviral vectors are delivered to cells in their immobilized form on microparticles, they can transduce cells because the microparticle makes direct and stable contact with the cell surface and enables a secondary interaction of the viral penton base with cellular integrins for adenovirus internalization into the cells independently of primary CAR binding (figure 3.8) [82]. As a result of the conditional transduction in the encoded viral micropatch-based gene delivery system, transduction occurs only in the micropatched cells, while transduction in cells outside the micropatch is severely suppressed even if some of the vectors are released into the medium from the micropatch, thus resulting in highly localized gene delivery only under the micropatch.

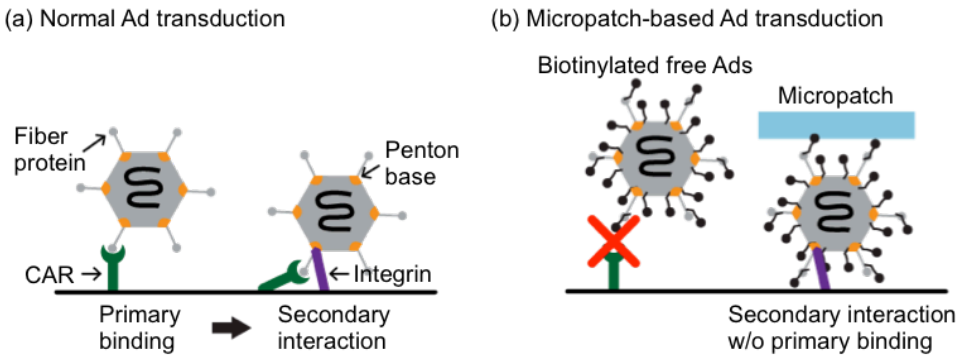

Figure 3.8 Comparison of adenoviral transduction: (a) CAR-dependent normal Ad transduction; (b) CAR-independent micropatch-based Ad transduction.

3.3.3 Transduction of an Adenoviral Receptor-deficient Cell Line

The CAR-independent transduction property of the encoded viral micropatch also makes CAR-negative cell lines susceptible to adenoviral gene delivery. This feature is investigated by comparing adenovirus transduction of the CAR-positive U-2 OS cell line with transduction of the CAR-negative RD (rhabdomyosarcoma) cell line [83]. U-2 OS and RD cell lines are cultured using McCoy's 5A medium and Dulbecco's Modified Eagle's Medium (DMEM), respectively, and incubated at 37 °C in 5% CO_2 for adenovirus transduction. Both media are supplemented with 10% foetal bovine serum and 1% penicillin-streptomycin. Each cell line is seeded at a density of 8,000 cells per well in an optically clear-bottomed 96-well plate and incubated overnight in a CO_2 chamber. Then, free Ad-RFP vectors with 50 MOI and square Ad-RFP micropatches are introduced into proper wells to investigate transduction of each cell line.

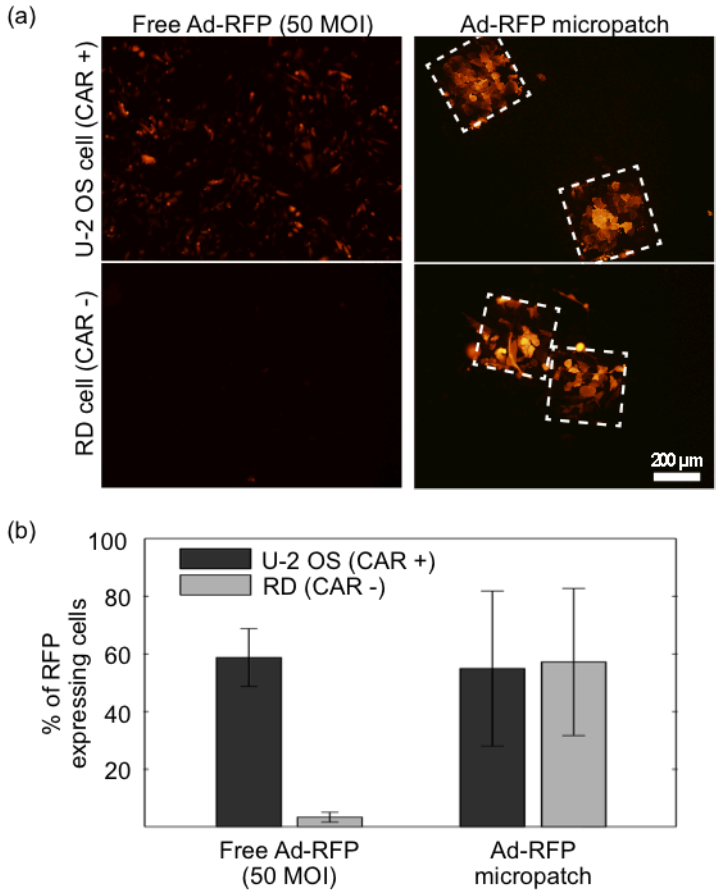

Figure 3.9 CAR-independent transduction with the encoded viral micropatch: (a) Fluorescence micrographs of U-2 OS (CAR-positive) and RD (CAR-negative) cells expressing RFP delivered using free adenoviral vectors (left column) and using Ad-RFP micropatches (right column, micropatches are indicated with white dashed lines); (b) Percentage of RFP expressing cells in (a). The error bars represent the standard deviation of the mean determined from 4 microscopic views for free Ad-RFP and 12 micropatches for each cell line.

The transduction efficiencies of free Ad-RFP particles and micropatches for the two cell lines are investigated by observing RFP expression (figure 3.9(a)). The

percent of RFP expressing RD cells is approximately 10-fold lower compared to U-2 OS cells when transduced by free viral particles (non-biotinylated), while expression increases significantly up to the level of U-2 OS cells when the viral micropatch is used for transduction (figure 3.9(b)). As mentioned above, this is possible because the microparticles mediate direct, stable contact of the adenoviral vectors with the cell surface. This CAR-independent transduction could be used to expand the list of available cell types for cell-based assays using adenoviral-mediated gene delivery.

3.3.4 Transduction Efficiency of the Encoded Viral Micropatch

In general, adenoviral vectors offer high transduction efficiency to a wide range of host cell types and this is one of the main reasons why many researchers use them for the gene delivery experiments. In this section, the transduction efficiency of the type 2 encoded viral micropatch is estimated and compared to that of free adenoviral vectors. For this purpose, the number of the immobilized adenoviral vectors on a micropatch is measured because the transduction efficiency is calculated as the percentage of transduced cells among total cells with respect to the number of viral vectors used. My approach for the titration of the amount of adenoviral vectors is to count the number of adenoviral DNAs by quantitative real-time polymerase chain reaction (qPCR), which amplifies and quantifies a targeted DNA molecule.

For the qPCR of the adenoviral DNA, adenoviral capsid proteins should be denaturized to extract the adenoviral genomic DNA. Pasteurization method is

applied to destruct the adenoviral vectors because it is simple and effective for non-enveloped viruses [84]. In this method, the denaturation of the adenoviral vectors are performed by incubating the vectors at 60 °C for 8 hours and confirmed by observing no transduction of cells with the denaturized vectors (figure 3.10).

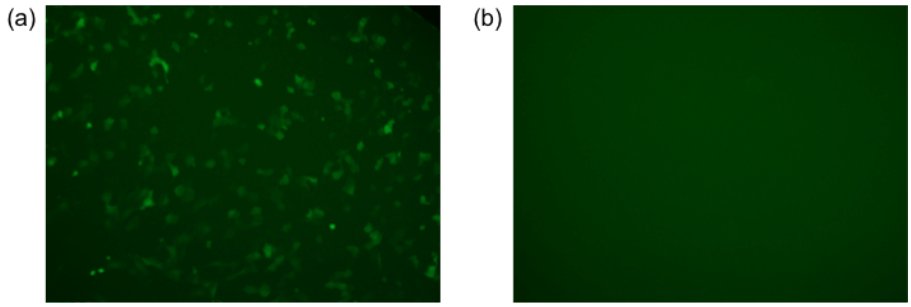

Figure 3.10 GFP expression in U-2 OS cells transduced with Ad-GFPs: (a) without denaturation; (b) with denaturation at 60 °C for 8 hours.

The adenoviral DNA templates for the qPCR are prepared separately to obtain a standard curve of known amounts of adenoviral vectors and to measure unknown amount of the immobilized vectors on the micropatch. For the standard curve, Ad-RFP vector stock with a titer of 10^{10} pfu/ml is denaturized with the above method and then, diluted with nuclease free water to have 10^9, 10^8, 10^7, and 10^6 pfu/ml stocks as well. For the micropatch, a few amount of square Ad-RFP micropatches are dispensed in a well of 96-well plate filled 100 µl of nuclease free water and counted using an optical microscope. A master mix for the qPCR is prepared as listed in table 3.1. The volumes are for a single reaction. Forward and reverse

primers are designed to target the human adenovirus type 5 sequence and produce amplicons with the length of 133 base pairs (bp).

Table 3.1 Components of the master mix for the qPCR

Components	Volume (µl)
Nuclease free water	15.25
5X KAPA HiFi fidelity buffer	5
10 mM dNTP mix	0.75
Forward primer (10 µM) (5'-CATGTCCCTGACTCGCATGT-3')	0.75
Reverse primer (10 µM) (5'-GCTCAAAAGCATGCCTACGG-3')	0.75
KAPA HiFi HotStart DNA polymerase (1 U/µl)	0.5
SYBR Green I	1
Total	24

In each reaction, 1 µl of adenoviral DNA is used. Each sample is run triplicate. After gently shaking and centrifuging, the tubes are placed in the thermal cycler (Applied Biosystems 7500 Fast Real-time PCR system). Then, the machine is programmed as follows: 1) initial denaturation for 5 min at 95 °C for one cycle, 2) denaturation for 20 sec at 98 °C, 3) annealing for 15 sec at 98 °C, 4) elongation for 20 sec at 72 °C, 5) repeat steps from 2) and 4) for 35 total cycle, and 6) final elongation for 3 min at 72 °C. The standard curve of the known amount of vectors and the interpolation of the unknown amount of vectors are shown in figure 3.11.

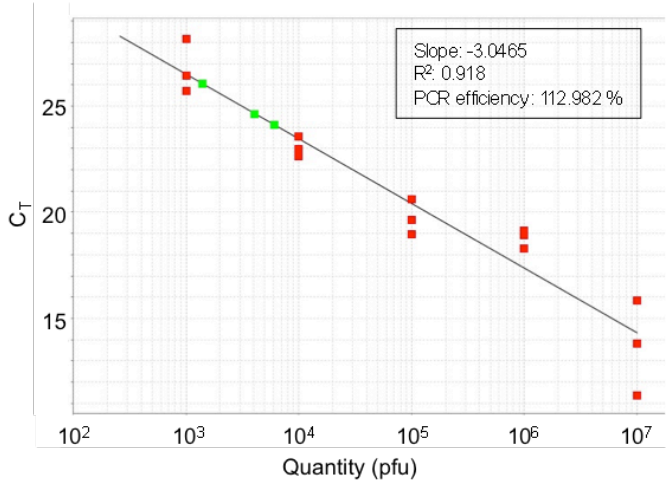

Figure 3.11 The qPCR standard curve of known amount of adenoviral vectors (red dots) and the interpolation of unknown amount of adenoviral vectors (green dots).

By considering the qPCR result and the dimension of the square micropatch together, the number of adenoviral vectors immobilized on a flat surface, which will face cells, is calculated as shown in figure 3.12.

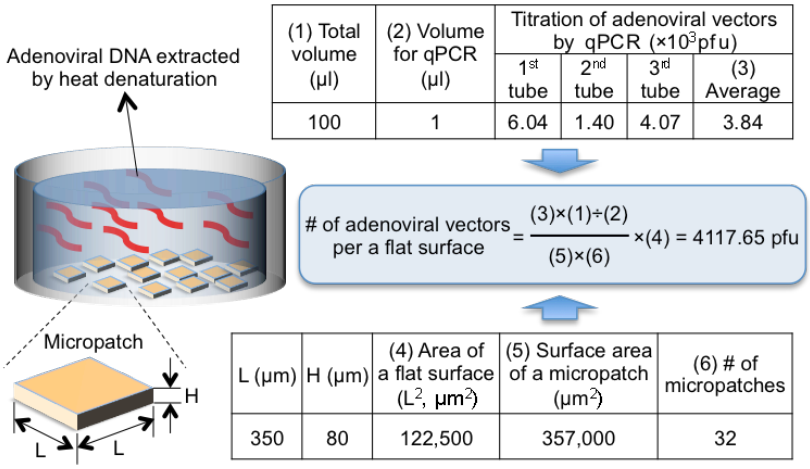

(1) Total volume (μl)	(2) Volume for qPCR (μl)	Titration of adenoviral vectors by qPCR (×10³pfu)			
		1st tube	2nd tube	3rd tube	(3) Average
100	1	6.04	1.40	4.07	3.84

$$\text{\# of adenoviral vectors per a flat surface} = \frac{(3)\times(1)\div(2)}{(5)\times(6)} \times (4) = 4117.65 \text{ pfu}$$

L (μm)	H (μm)	(4) Area of a flat surface (L^2, μm^2)	(5) Surface area of a micropatch (μm^2)	(6) # of micropatches
350	80	122,500	357,000	32

Figure 3.12 Calculation of the number of adenoviral vectors immobilized on the micropatch based the result of the qPCR.

Finally, in order to compare the transduction efficiencies of free Ad-RFP and the square Ad-RFP micropatch, U-2 OS cells are transduced using both adenoviral vector delivery methods and the percentage of cells expressing RFP is obtained (table 3.2). The number of total cells under a micropatch is 83.21 and thus, MOI is 49.49 when adenoviral vectors are delivered with the encoded viral micropatch. When compared the transduction efficiency of free adenoviral vectors at 50 MOI, which is 60.24 %, the encoded viral micropatch shows similar level of transduction efficiency. That is, the encoded viral micropatch offers normal level of transduction efficiency even though the immobilized adenoviral vectors lose their infectivity by the biotinylation.

Table 3.2 Comparison of the transduction efficiencies of the encoded viral micropatch and free adenoviral vector.

	Micropatch	Free adenoviral vector						
MOI	49.49	1	5	10	50	100	500	1000
Transduction efficiency (%)	57.94	3.79	7.94	14.68	60.24	77.17	99.88	100.00

3.4 Conclusion

In chapter 3, the localized gene delivery of both types of the encoded viral micropatch was evaluated. Cells grown in a well of a 96-well plate were transduced with the encoded viral micropatch fabricated with adenoviral vectors carrying fluorescence protein genes and then, the expression of fluorescence proteins in cells both under and outside the micropatch was quantitatively analyzed. This showed that the type 2 encoded viral micropatch offered highly localized gene delivery while the type 1 encoded viral micropatch did not. The high rate of localization of the type 2 encoded viral micropatch is owing to the conditional transduction of the biotinylated adenoviral vectors. The biotinylated adenoviral vectors lose their infectivity because the primary binding to the adenovirus cell receptor (CAR) is prevented while they can transduce cells when delivered closely to cells in the micropatch form, which enables the secondary interaction with cell surface integrins. By utilizing this CAR-independent transduction, the type 2 encoded viral micropatch transduced a CAR-deficient cell line. Also, the transduction efficiency of the type 2 encoded viral micropatch examined by qPCR is similar with that of free adenoviral vectors even though the immobilized vectors are biotinylated.

Chapter 4

Multiplex GPCR Internalization Assay

This chapter introduces a multiplexed GPCR internalization assay using the localized multiplex adenoviral gene delivery system. The development of high-throughput cell-based GPCR functional assays is very important for screening large compound libraries in the drug discovery process and ligand-induced receptor internalization assays have broad applicability to various GPCR subfamilies among several GPCR assay formats. However, high-content imaging is required for fluorescence-based intracellular measurement of receptor internalization. To address this issue, I fabricate three types of encoded viral micropatches with adenoviral vectors bearing GFP-tagged GPCR genes and the responses of multiple GPCRs against one ligand treatment is acquired in one reaction site by achieving simultaneous expression of multiple GPCRs with the fabricated viral micropatches

in a cell monolayer cultured in a well of a 96-well plate. High-content analysis of this micropatch-based multiplexed assay shows comparable results in the receptor internalization with the conventional singlet assay using free adenoviral vectors while reducing the number of pipetting actions.

4.1 G Protein-coupled Receptor (GPCR)

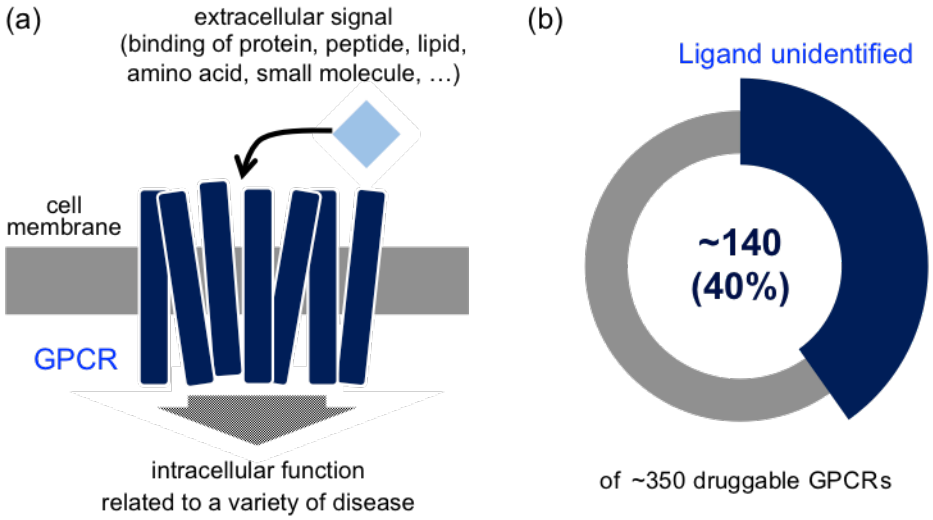

Figure 4.1 G protein-coupled receptor: (a) an illustration of the structure and signal transduction of GPCRs; (b) the statistics of known and orphan GPCRs.

GPCRs are the largest family of cell membrane-signaling proteins that transmit extracellular signals into the cell (figure 4.1a). A huge variety of endogenous ligands from small molecules to proteins can bind to their specific GPCRs and these bindings trigger many intracellular functions. Because these signal transductions are related to many physiological processes or diseases, GPCRs have been significant and important targets in pharmaceutical industry, accounting for about one-third of marketed drugs [85, 86]. Endogenous ligands have been proposed for more than 200 GPCRs; however, over 100 GPCRs still remain orphan, which means their

endogenous ligands are not yet identified (figure 4.2b). Therefore, the development of high-throughput functional screenings for both known and orphan GPCRs is highly required to identify new drug candidates and targets in GPCR-targeted drug discovery process [87].

After activation of the receptor by their ligands, GPCRs become phosphorylated and desensitized, and subsequently internalized into endocytotic compartments in cells. Internalized receptors are then either recycled back to the plasma membrane of the cell, or transferred to lysosomes for degradation. Exposure of a GPCR to its natural ligand internalizes most GPCRs, which can be observed with GFP-tagged receptors, thereby enabling the development of cell-based high throughput screening assays of GPCR internalization (figure 4.2) [85, 88].

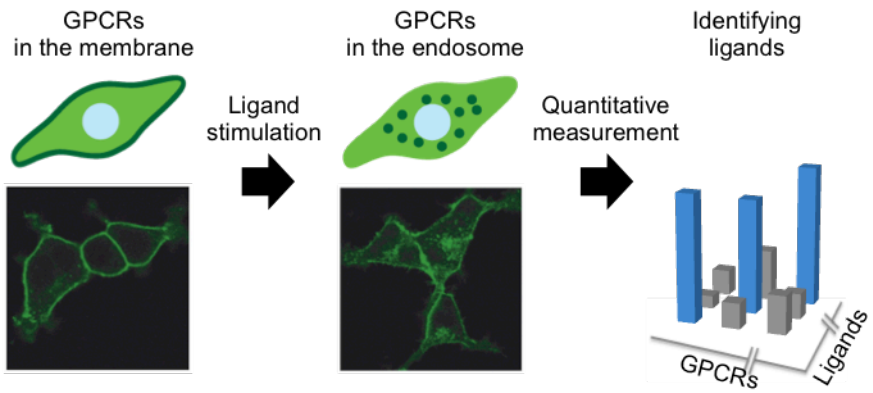

Figure 4.2 Ligand-induced GPCR internalization and fluorescence-based detection.

4.2 Materials for the Assay

4.2.1 GPCR Adenoviral Vectors

Three GPCR genes are targeted for the demonstration of multiplexed assay: galanin receptor 1 (GALR1), alpha-2B adrenergic receptor (ADRA2B), and histamine receptor H1 (HRH1). Adenoviral vectors expressing GFP-tagged GPCR (Ad-GALR1-GFP, Ad-ADRA2B-GFP, and Ad-HRH1-GFP) are purchased from Boram Pharm. Co., Ltd. (Seoul, Korea). GFP tagging is for visualizing the GPCR internalization in living cells. All viruses are prepared in PBS.

4.2.2 Ligands

Human galanin (1-30) (Tocris Bioscience), UK 14,304 (Sigma-Aldrich), and histamine (Sigma-Aldrich) are used as ligands for GPCR internalisation. Ligand solutions are prepared at a concentration of 200 μM in serum-free McCoy's 5A medium with 10% dimethyl sulfoxide (DMSO). Serum-free McCoy's 5A medium with 10% DMSO is prepared as a negative control ligand.

4.2.3 Cell Culture

U-2 OS is cultured using McCoy's 5A medium, and incubated at 37 °C in 5% CO_2 for adenovirus transduction. This medium is supplemented with 10% foetal bovine serum and 1% penicillin-streptomycin.

4.3 Conventional GPCR Internalization Assay

Before conducting multiplex GPCR internalization assays using the encoded viral micropatch, I carry out GPCR internalization assay using a conventional method, which uses one type of viral vectors in each well of a 96-well microplate. This singlet assay results will be used as reference data to evaluate the assay quality of the encoded viral micropatch-based multiplex GPCR internalization assays.

4.3.1 Assay Procedure

U-2 OS cells are seeded at a density of 8,000 cells per well in an optically clear-bottomed 96-well plate and incubated overnight in a CO_2 chamber. To express a GPCR in cells, each Ad-GPCR-GFP solution is introduced into the separated wells. For testing the receptor internalization induced by three ligands and one negative control buffer, at least 4 wells are used for each viral vector. By considering both high transduction and cytotoxicity, I use 10 MOI for Ad-GALR1-GFP and Ad-ADRA2B-GFP, and 20 MOI for Ad-HRH1-GFP (figure 4.3).

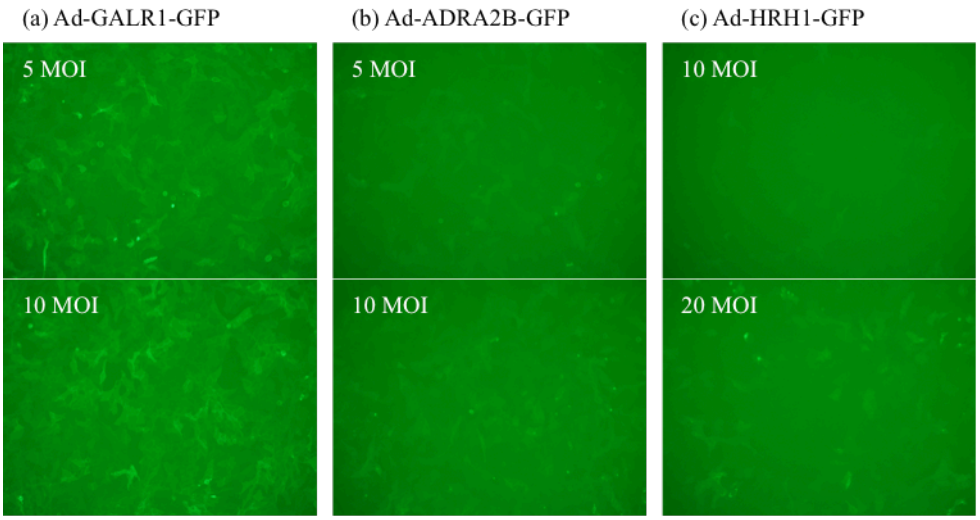

Figure 4.3 A MOI test for each Ad-GPCR-GFP: (a) Ad-GALR1-GFP; (b) Ad-ADRA2B-GFP; (c) Ad-HRH1-GFP.

After a 40-hour incubation, GPCR expressions are confirmed through GFP observation in the cells. Then, the infected cells are washed with PBS three times and incubated in 95 μL of serum-free McCoy's 5A medium for 1 hour.

Three kind of ligand (galanin, UK 14,304, and histamine) solutions are prepared at a concentration of 200 μM in serum-free McCoy's 5A medium with 10% DMSO. The cells are stimulated with either 10 μM of one of three ligands or 0.5% DMSO by adding 5 μL of the ligand solution or serum-free McCoy's 5A medium with 10% DMSO to the appropriated wells for 1 hour. The medium is then removed, and the cells are washed with PBS three times. The cells are fixed in 100 μL of PBS with 2% formaldehyde at room temperature for 20 min. After 3 washes with PBS,

the nuclei are stained with 100 µL of 2 µg/mL Hoechst 33342 in PBS for 10 min in a CO_2 incubator. Finally, each well is prepared for confocal imaging by filling with 200 µL of PBS after 3 washes with PBS.

Imaging of the assay plates is performed using a confocal laser scanning microscope (TCS SP5, Leica Microsystems). GFP indicating the expression of GPCRs is excited with a 488 nm laser line, and the emission is detected with a 510-530 nm bandpass filter. A 405 nm laser line is used to excite the stained nuclei, and a 440-465 nm bandpass filter is used to detect the emission.

Lastly, in order to quantify the GPCR internalisation, the acquired images are analysed using an open-source cell image analysis software (CellProfiler [89], http://www.cellprofiler.org) (figure 4.4).

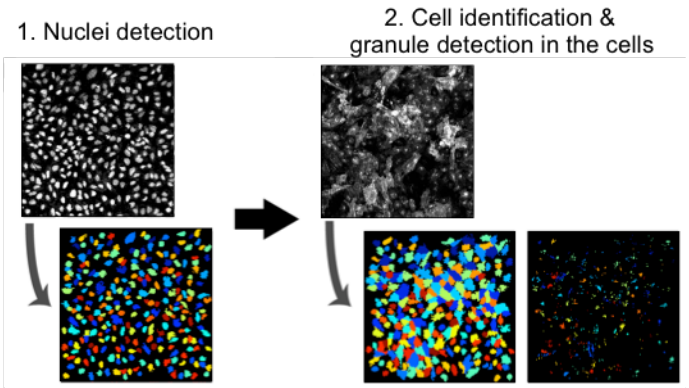

Figure 4.4 The image processing steps for quantitative measurement of the receptor internalization in a conventional singlet assay using a CellProfiler.

In detail, the nuclei are identified using a specified intensity threshold, size, and shape in the blue channel image. Cells are then identified by outward growth from nuclei until reaching the edge of the image threshold or a neighbour in the green channel. Granules, which are identified as accumulations of green fluorescence created by the internalised receptors, are detected using size and intensity thresholds. The fluorescent intensity of cells and granules are measured to calculate receptor internalisation ($F_{granule}$) as follows.

$$F_{granule} = \frac{Sum\ of\ pixel\ values\ corresponding\ to\ valid\ granules\ in\ dilated\ mask\ region}{Sum\ of\ pixel\ values\ in\ dilated\ mask\ region} \times 1000 \quad (4.1)$$

4.3.2 Assay Result

Figure 4.5 shows representative images of every combination of GPCR and ligand tested in this assay. Receptor internalisation, which is indicated by the accumulation of green fluorescence within centralised intracellular locations, is greatest in the pairs of receptor and its well-known ligand (galanin for GALR1, UK 14,304 for ADRA2B, and histamine for HRH1). The quantitative measurements of the receptor internalization is obtained using the aforementioned image processing method and displayed in figure 4.6.

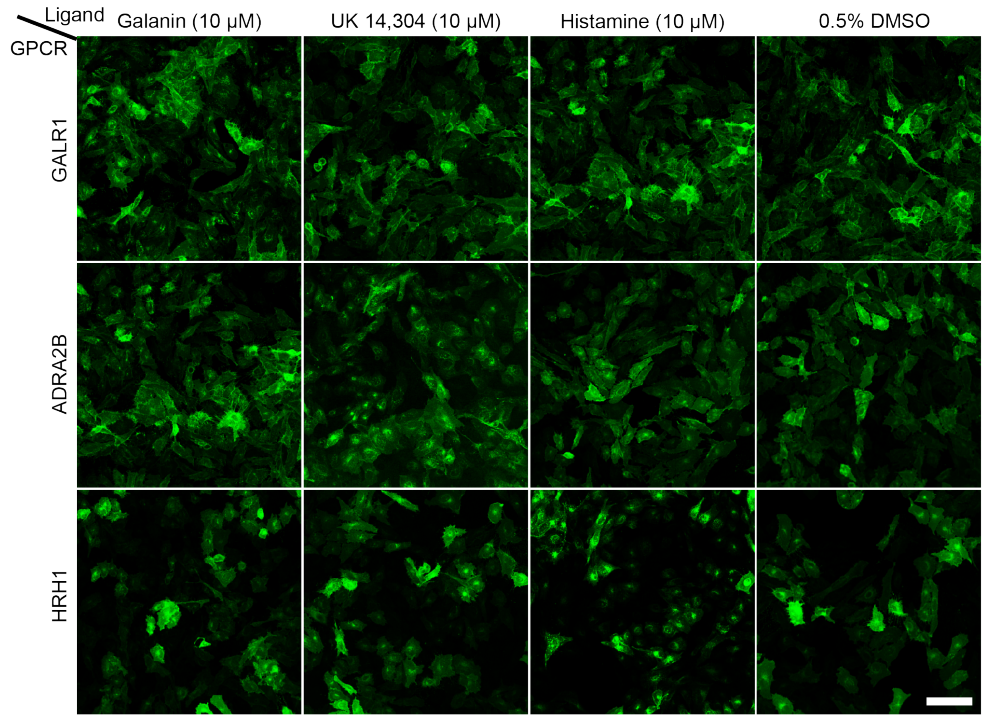

Figure 4.5 A conventional singlet GPCR internalization assay using free Ad-GPCR-GFPs (scale bar: 100 μm).

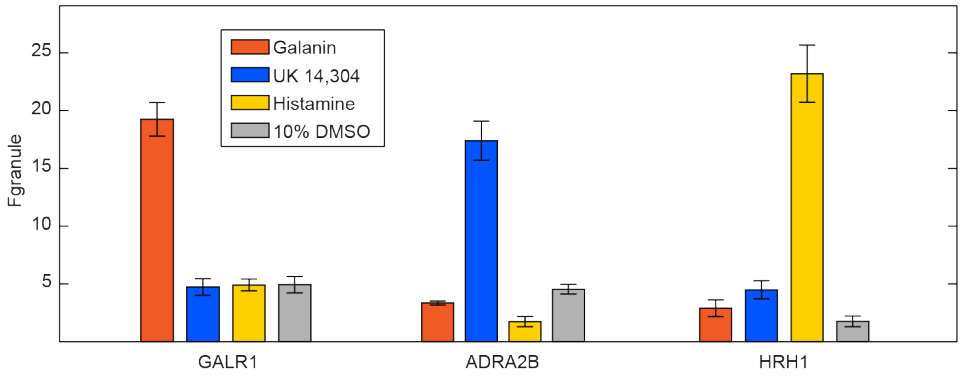

Figure 4.6 Quantitative measurements of the receptor internalization in conventional singlet assays.

4.4 Multiplex GPCR Internalization Assay

4.4.1 Preparation of Encoded Viral Micropatches

I prepare three types of encoded viral micropatches to deliver GPCR genes to cultured cell monolayers. Circular, square, and star-shaped microparticles are used to immobilize adenoviral vectors bearing genes for the GFP-tagged galanin receptor 1 (Ad-GALR1-GFP), alpha-2B adrenergic receptor (Ad-ADRA2B-GFP), and histamine receptor H1 (Ad-HRH1-GFP), respectively. The shape-coded polymer microparticles are fabricated with the effective diameter of 350 μm to have 80-100 cells under each micropatch and the thickness of 80 μm. Between two viral immobilization methods described in chapter 2, the particle-biotin-avidin-biotin-adenovirus configuration is used for the preparation of Ad-GPCR-GFP micropatches.

4.4.2 Assay Procedure

The assay procedure of multiplex GPCR internalization assay using the encoded viral micropatch is same with a conventional singlet assay, which consists of 5 steps: 1) cell seeding and GPCR gene delivery, 2) ligand treatment, 3) post processing including cell fixation and nuclei staining, 4) high-content imaging, and 5) image analysis for the quantitative measurement of the receptor internalization (figure 4.7).

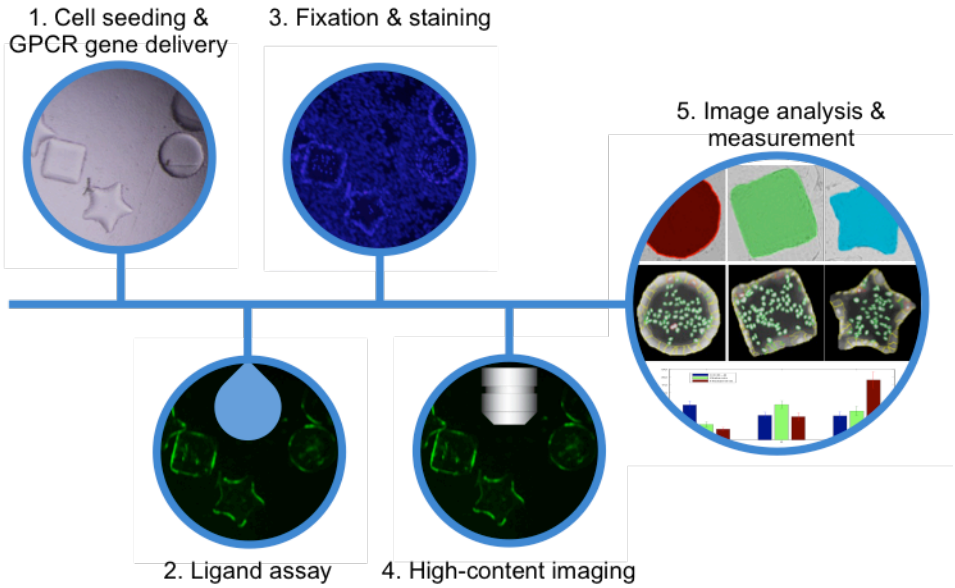

Figure 4.7 The assay procedure of multiplex GPCR internalization assays using the encoded viral micropatch.

However, in the multiplex assay, there are small changes for viral delivery, ligand treatment, image acquisition, and image processing. The number of pipetting actions for viral delivery and ligand treatment is reduced proportionately to the number of GPCRs because a heterogeneous mixture of the micropatches are delivered to cells by a single pipetting action to achieve simultaneous expression of these GPCRs at one reaction site. In the case of image acquisition, transmitted light channel images are additionally acquired using a confocal laser scanning microscope to obtain images showing the shapes of the micropatches.

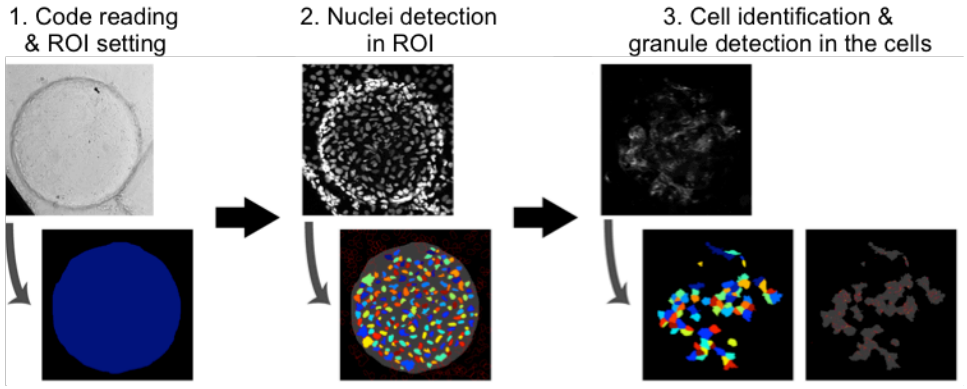

Figure 4.8 The image processing steps for quantitative measurement of the receptor internalization in the encoded viral micropatch-based muliplex assay using a CellProfiler.

For image processing to quantify the GPCR internalisation, the shape detection of the micropatch is added prior to the nuclei detection (figure 4.8). In addition, the region of the recognized micropatch is used as the region of interest (ROI) for following image processing steps in order to include only cells under the micropatch.

4.4.3 Assay Result

Figure 4.9 shows representative images of every combination of GPCR and ligand tested in this assay system. Receptor internalisation, which is indicated by the accumulation of green fluorescence within centralised intracellular locations, is greatest in the pairs of receptor and its well-known ligand (galanin for GALR1, UK 14,304 for ADRA2B, and histamine for HRH1) as shown in the insets. Quantitative values for internalisation, $F_{granule}$ are plotted in figure 4.10. As a reference for GPCR

internalisation, the $F_{granule}$ values obtained from the conventional singlet assay using free adenoviral particles are also plotted. The assay using the encoded viral micropatches shows comparable $F_{granule}$ values with the reference assay.

Compared to the conventional GPCR internalisation assay, the micropatch-based approach does not require any complex changes of assay procedure such as cell preparation, ligand activation, cell fixation, and staining as well as high-content cellular imaging, while the number of pipetting actions for delivering adenoviral vectors and ligands are reduced proportionately to the number of target proteins. Although a detection step for the shape codes is added to the image analysis process, it requires relatively simple image processing and only a short processing time. Therefore, we can conclude that it is feasible to use our encoded viral micropatch system in high-throughput image-based GPCR internalisation assays.

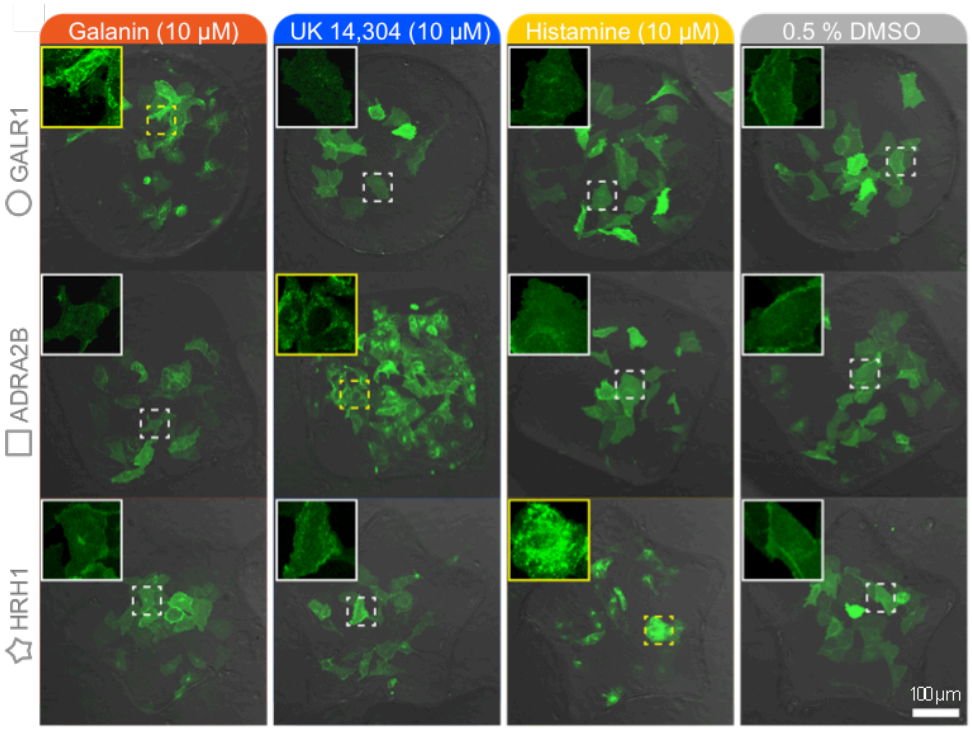

Figure 4.9 A multiplex GPCR internalization assay using the encoded viral micropatches. Overlaid confocal laser scanning microscope images of GPCR internalization by ligand activation: Ad-GALR1-GFP on the circular micropatch, Ad-ADRA2B-GFP on the square micropatch, and Ad-HRH1-GFP on the star micropatch.

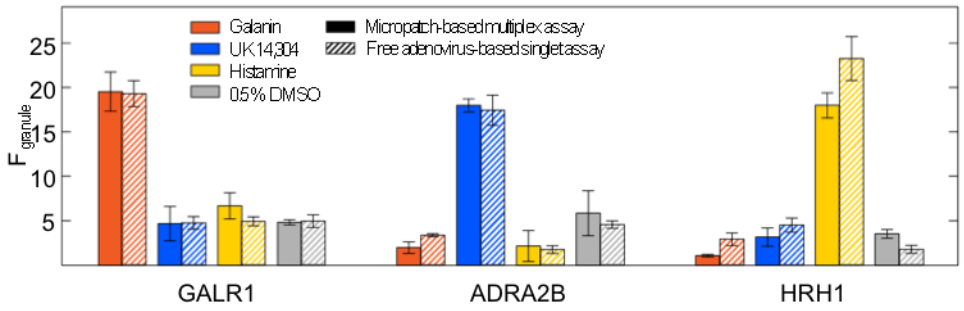

Figure 4.10 Quantitative measurements of the receptor internalization in the encoded viral micropatch-based multiplex assays (solid bars). The conventional singlet assay results using free adenoviral particles are displayed as bars with diagonal lines for reference.

4.5 Conclusion

In chapter 4, a multiplex GPCR internalization assay is demonstrated using the encoded viral micropatches developed in previous chapters. Successive achievement of multiplex expression of GFP-tagged GPCRs in cells cultured in a well of a 96-well plate using the encoded viral micropatch technology enables high-throughput screening of GPCR-ligand interactions in a high-content manner. This multiplex assay using the encoded viral micropatches gives comparable results to a conventional singlet assay using free adenoviral vectors while using only 4 wells for 12 combinations of GPCR-ligand interactions instead of 12 separate wells, without any changes to the high-content assay procedure. As demonstrated in this assay, the encoded viral micropatch system will accelerate and enrich cell-based functional assays for drug discovery.

Conclusion

In this dissertation, I developed the first microparticle-mediated adenoviral gene delivery method that fully supports simultaneous high-throughput and high-content cell-based assays. To achieve these capabilities, I proposed the 'encoded viral micropatch', which means an adenoviral vector-immobilized microparticle with a 2D shape code that can be used like a patch on 2D-cultured cells.

To produce the encoded viral micropatches, polymeric microparticles with distinct 2D shape codes were fabricated via photopolymerisation. The adenoviral vectors were then immobilized on the shape-coded microparticles to achieve one-to-one correspondence between the genetic vectors and the shape codes using two approaches: 1) direct conjugation of the carboxyl groups on the microparicles and the primary amine groups on the viral capsid via EDC plus Sulfo-NHS reaction, 2) avidin-mediated combination after the biotinylation of both the microparticles and adenoviral vectors.

In this study, a heterogeneous mixture of encoded viral micropatches was pipetted on a cell monolayer to create cell clusters with distinct protein expressions by way of localized transduction of the cells only under the micropatches. Especially, by using the encoded viral micropatch fabricated via avidin-biotin interaction, highly localized viral gene delivery was achieved utilizing the infection deficiency of the biotinylated adenoviruses in their free form and recovery of infectivity when delivered to the cells in the microparticle-immobilized form. This conditional transduction resulted in transduction of the cells by the encoded viral micropatch regardless of whether the cells expressed the primary adenovirus binding receptor.

Using this multiplex gene delivery system, I demonstrated a multiplex GPCR internalization assay that requires fluorescence-based high-content imaging to show the compatibility of the encoded viral micropatches with high-throughput, high-content cell-based assays. This encoded viral micropatch system will accelerate and enrich cell-based functional assays for drug discovery, as demonstrated in the multiplexed GPCR internalisation assay developed.

Bibliography

[1] R. Zang, D. Li, I.-C. Tang, et al., "Cell-based assays in high-throughput screening for drug discovery," *International Journal of Biotechnology for Wellness Industries*, vol. 1, no. 1, pp. 31-51, 2012.

[2] W. F. An, N. Tolliday, "Cell-based assays for high-throughput screening," *Molecular Biotechnology*, vol. 45, no. 2, pp. 180-186, 2010.

[3] E. Michelini, L. Cevenini, L. Mezzanotte, et al., "Cell-based assays: Fuelling drug discovery," *Analytical and Bioanalytical Chemistry*, vol. 398, no. 1, pp. 227-238, 2010.

[4] E. Palmer. *Cell-based microarrays: Review of applications, developments and technological advances*. (Springer Science & Business Media, 2014).

[5] R. S. Ames, Q. Lu, "Viral-mediated gene delivery for cell-based assays in drug discovery," *Expert Opinion on Drug Discovery*, vol. 4, no. 3, pp. 243-256, 2009.

[6] M. T. Lotze, T. A. Kost, "Viruses as gene delivery vectors: Application to gene function, target validation, and assay development," *Cancer Gene Therapy*, vol. 9, no. 8, pp. 692-699, 2002.

[7] O. E. Beske, S. Goldbard, "High-throughput cell analysis using multiplexed array technologies," *Drug Discovery Today*, vol. 7, no. 18, pp. S131-S135, 2002.

[8] S. A. Sundberg, "High-throughput and ultra-high-throughput screening: Solution- and cell-based approaches," *Current Opinion in Biotechnology*, vol. 11, no. 1, pp. 47-53, 2000.

[9] J. Denyer, J. Worley, B. Cox, et al., "Hts approaches to voltage-gated ion channel drug discovery," *Drug Discovery Today*, vol. 3, no. 7, pp. 323-332, 1998.

[10] J. E. González, K. Oades, Y. Leychkis, et al., "Cell-based assays and instrumentation for screening ion-channel targets," *Drug Discovery Today*, vol. 4, no. 9, pp. 431-439, 1999.

[11] T. R. Sharif, M. Sharif, "A novel approach for examining the anti-proliferative effect of protein kinase c inhibitors against human astrocytoma cells," *International journal of oncology*, vol. 13, no. 4, pp. 685-777, 1998.

[12] T. R. Sharif, M. Sharif, "A high throughput system for the evaluation of protein kinase c inhibitors based on elk1 transcriptional activation in human astrocytoma cells," *International journal of oncology*, vol. 14, no. 2, pp. 327-362, 1999.

[13] J. Bedard, S. May, D. Barbeau, et al., "A high throughput colorimetric cell proliferation assay for the identification of human cytomegalovirus inhibitors," *Antiviral Research*, vol. 41, no. 1, pp. 35-43, 1999.

[14] K. A. Giuliano, J. R. Haskins, D. L. Taylor, "Advances in high content screening for drug discovery," *Assay and drug development technologies*, vol. 1, no. 4, pp. 565-577, 2003.

[15] P. Lang, K. Yeow, A. Nichols, et al., "Cellular imaging in drug discovery," *Nature Reviews Drug Discovery*, vol. 5, no. 4, pp. 343-356, 2006.

[16] F. Zanella, J. B. Lorens, W. Link, "High content screening: Seeing is believing," *Trends in Biotechnology*, vol. 28, no. 5, pp. 237-245, 2010.

[17] M. Götte, D. Gabriel. in *Drug discovery and development - present and future* (ed Izet Kapetanović) Ch. 14, (InTech, 2011).

[18] V. Starkuviene, R. Pepperkok, "The potential of high-content high-throughput microscopy in drug discovery," *British Journal of Pharmacology*, vol. 152, no. 1, pp. 62-71, 2007.

[19] Y. Futamura, M. Kawatani, S. Kazami, et al., "Morphobase, an encyclopedic cell morphology database, and its use for drug target identification," *Chemistry*

& Biology, vol. 19, no. 12, pp. 1620-1630, 2012.

[20] S. N. Bailey, S. M. Ali, A. E. Carpenter, et al., "Microarrays of lentiviruses for gene function screens in immortalized and primary cells," *Nature Methods*, vol. 3, no. 2, pp. 117-122, 2006.

[21] R. Carbone, L. Giorgetti, A. Zanardi, et al., "Retroviral microarray-based platform on nanostructured tio2 for functional genomics and drug discovery," *Biomaterials*, vol. 28, no. 13, pp. 2244-2253, 2007.

[22] A. Oehmig, A. Klotzbucher, M. Thomas, et al., "A novel reverse transduction adenoviral array for the functional analysis of shrna libraries," *BMC Genomics*, vol. 9, no. pp. 441, 2008.

[23] K. C. Wood, D. J. Konieczkowski, C. M. Johannessen, et al., "Microscale screening reveals genetic modifiers of therapeutic response in melanoma," *Science Signaling*, vol. 5, no. 224, pp. rs4, 2012.

[24] D. Castel, A. Pitaval, M.-A. Debily, et al., "Cell microarrays in drug discovery," *Drug Discovery Today*, vol. 11, no. 13–14, pp. 616-622, 2006.

[25] J. Reymann, N. Beil, J. Beneke, et al., "Next-generation 9216-microwell cell arrays for high-content screening microscopy," *Biotechniques*, vol. 47, no. pp. 877-878, 2009.

[26] J. P. Nolan, L. A. Sklar, "Suspension array technology: Evolution of the flat-array paradigm," *Trends in Biotechnology*, vol. 20, no. 1, pp. 9-12, 2002.

[27] R. Wilson, A. R. Cossins, D. G. Spiller, "Encoded microcarriers for high-throughput multiplexed detection," *Angewandte Chemie International Edition*, vol. 45, no. 37, pp. 6104-6117, 2006.

[28] F. Fayazpour, B. Lucas, R. E. Vandenbroucke, et al., "Evaluation of digitally encoded layer-by-layer coated microparticles as cell carriers," *Advanced Functional Materials*, vol. 18, no. 18, pp. 2716-2723, 2008.

[29] D. J. Beebe, J. S. Moore, J. M. Bauer, et al., "Functional hydrogel structures for autonomous flow control inside microfluidic channels," *Nature*, vol. 404, no. 6778, pp. 588-590, 2000.

[30] D. Dendukuri, D. C. Pregibon, J. Collins, et al., "Continuous-flow lithography

for high-throughput microparticle synthesis," *Nature Materials*, vol. 5, no. 5, pp. 365-369, 2006.

[31] D. C. Pregibon, M. Toner, P. S. Doyle, "Multifunctional encoded particles for high-throughput biomolecule analysis," *Science*, vol. 315, no. 5817, pp. 1393-1396, 2007.

[32] D. Dendukuri, S. S. Gu, D. C. Pregibon, et al., "Stop-flow lithography in a microfluidic device," *Lab on a Chip*, vol. 7, no. 7, pp. 818-828, 2007.

[33] H. Martinsson, T. Sandstrom, A. Bleeker, et al., "Current status of optical maskless lithography," *Journal of Micro/Nanolithography, MEMS, and MOEMS*, vol. 4, no. 1, pp. 011003-011003-011015, 2005.

[34] S. E. Chung, W. Park, H. Park, et al., "Optofluidic maskless lithography system for real-time synthesis of photopolymerized microstructures in microfluidic channels," *Applied Physics Letters*, vol. 91, no. 4, pp. 041106-041103, 2007.

[35] S.-H. Song, K. Kim, S.-E. Choi, et al., "Fine-tuned grayscale optofluidic maskless lithography for three-dimensional freeform shape microstructure fabrication," *Optics Letters*, vol. 39, no. 17, pp. 5162-5165, 2014.

[36] S. E. Chung, S. A. Lee, J. Kim, et al., "Optofluidic encapsulation and manipulation of silicon microchips using image processing based optofluidic maskless lithography and railed microfluidics," *Lab on a Chip*, vol. 9, no. 19, pp. 2845-2850, 2009.

[37] F. Michiels, H. van Es, L. van Rompaey, et al., "Arrayed adenoviral expression libraries for functional screening," *Nature Biotechnology*, vol. 20, no. 11, pp. 1154-1157, 2002.

[38] V. N. Ngo, R. E. Davis, L. Lamy, et al., "A loss-of-function rna interference screen for molecular targets in cancer," *Nature*, vol. 441, no. 7089, pp. 106-110, 2006.

[39] *Viral-mediated gene delivery*, <http://www.sciencemag.org/site/products/posters/GeneDeliveryPoster.PDF%3E>.

[40] J.-H. Jang, D. V. Schaffer, L. D. Shea, "Engineering biomaterial systems to

enhance viral vector gene delivery," *Molecular Therapy*, vol. 19, no. 8, pp. 1407-1415, 2011.

[41] D. Dendukuri, P. Panda, R. Haghgooie, et al., "Modeling of oxygen-inhibited free radical photopolymerization in a pdms microfluidic device," *Macromolecules*, vol. 41, no. 22, pp. 8547-8556, 2008.

[42] P. M. O. Wong. in *Tablets & Capsules* Vol. 9 28-33 (CSC Publishing Inc., 2011).

[43] F. Fayazpour, B. Lucas, N. Huyghebaert, et al., "Digitally encoded drug tablets to combat counterfeiting," *Advanced Materials*, vol. 19, no. 22, pp. 3854-3858, 2007.

[44] C. Huang, B. Lucas, C. Vervaet, et al., "Unbreakable codes in electrospun fibers: Digitally encoded polymers to stop medicine counterfeiting," *Advanced Materials*, vol. 22, no. 24, pp. 2657-2662, 2010.

[45] K. Braeckmans, S. C. De Smedt, C. Roelant, et al., "Encoding microcarriers by spatial selective photobleaching," *Nature Materials*, vol. 2, no. 3, pp. 169-173, 2003.

[46] H. Kato, K. T. Tan, "Pervasive 2d barcodes for camera phone applications," *Pervasive Computing, IEEE*, vol. 6, no. 4, pp. 76-85, 2007.

[47] P. Premaratne, F. Safaei, "2d barcodes as watermarks in image authentication," in *Computer and Information Science, 2007. 6th IEEE/ACIS International Conference on,* 11-13 July 2007, 2007, pp. 432-437.

[48] J. Z. Gao, L. Prakash, R. Jagatesan, "Understanding 2d-barcode technology and applications in m-commerce - design and implementation of a 2d barcode processing solution," in *Computer Software and Applications Conference, 2007. 31st Annual International,* 24-27 July 2007, 2007, pp. 49-56.

[49] K. W. Bong, S. C. Chapin, P. S. Doyle, "Magnetic barcoded hydrogel microparticles for multiplexed detection," *Langmuir*, vol. 26, no. 11, pp. 8008-8014, 2010.

[50] H. Lee, J. Kim, H. Kim, et al., "Colour-barcoded magnetic microparticles for multiplexed bioassays," *Nature Materials*, vol. 9, no. 9, pp. 745-749, 2010.

[51] S. C. Chapin, D. C. Pregibon, P. S. Doyle, "High-throughput flow alignment of barcoded hydrogel microparticles," *Lab on a Chip*, vol. 9, no. 21, pp. 3100-3109, 2009.

[52] W. Park, H. Lee, H. Park, et al., "Sorting directionally oriented microstructures using railed microfluidics," *Lab on a Chip*, vol. 9, no. 15, pp. 2169-2175, 2009.

[53] J. Wölcke, D. Ullmann, "Miniaturized hts technologies – uhts," *Drug Discovery Today*, vol. 6, no. 12, pp. 637-646, 2001.

[54] P. S. Dittrich, A. Manz, "Lab-on-a-chip: Microfluidics in drug discovery," *Nature Reviews Drug Discovery*, vol. 5, no. 3, pp. 210-218, 2006.

[55] G. M. Whitesides, "The origins and the future of microfluidics," *Nature*, vol. 442, no. 7101, pp. 368-373, 2006.

[56] W. Park, S. Han, S. Kwon, "Fabrication of membrane-type microvalves in rectangular microfluidic channels via seal photopolymerization," *Lab on a Chip*, vol. 10, no. 20, pp. 2814-2817, 2010.

[57] J. Hong, J. B. Edel, A. J. deMello, "Micro- and nanofluidic systems for high-throughput biological screening," *Drug Discovery Today*, vol. 14, no. 3–4, pp. 134-146, 2009.

[58] S. Pimputkar, J. S. Speck, S. P. DenBaars, et al., "Prospects for led lighting," *Nature Photonics*, vol. 3, no. pp. 2009.

[59] N. T. Tran, F. G. Shi, "Studies of phosphor concentration and thickness for phosphor-based white light-emitting-diodes," *Journal of Lightwave Technology*, vol. 26, no. pp. 3556-3559, 2008.

[60] W. D. Collins, M. R. Krames, G. J. Verhoeckx, et al. Using electrophoresis to produce a conformally coated phosphor-converted light emitting semiconductor. U.S. patent 6 576 488 (2003).

[61] Y. Jun-ho, S. Soo-Yeon, L. Seonghoon, et al., "Y[sub 3]al[sub 5]o[sub 12]:Ce[sub 0.05] phosphor coatings on gallium nitride for white light emitting diodes," *Journal of The Electrochemical Society*, vol. 150, no. 2, pp. H47-H52, 2003.

[62] B. Braune, K. Petersen, J. Strauss, et al., "A new wafer level coating technique

to reduce the color distribution of leds," in *Proc. SPIE 6486, Light-Emitting Diodes: Research, Manufacturing, and Applications XI,* San Jose, CA, Feb. 13, 2007, pp. 64860X.

[63] G. H. Negley, M. Leung. Methods of coating semiconductor light emitting elements by evaporating solvent from a suspension. U.S. patent 7 217 583 (2007).

[64] H.-T. Huang, C.-C. Tsai, Y.-P. Huang, "Conformal phosphor coating using pulsed spray to reduce color deviation of white leds," *Optics Express*, vol. 18, no. S2, pp. A201-A206, 2010.

[65] R. J. Fulton, R. L. McDade, P. L. Smith, et al., "Advanced multiplexed analysis with the flowmetrixtm system," *Clinical Chemistry*, vol. 43, no. 9, pp. 1749-1756, 1997.

[66] M. Han, X. Gao, J. Z. Su, et al., "Quantum-dot-tagged microbeads for multiplexed optical coding of biomolecules," *Nat Biotech*, vol. 19, no. 7, pp. 631-635, 2001.

[67] C. D. Keating, M. J. Natan, "Striped metal nanowires as building blocks and optical tags," *Advanced Materials*, vol. 15, no. 5, pp. 451-454, 2003.

[68] K. Braeckmans, S. C. De Smedt, M. Leblans, et al., "Encoding microcarriers: Present and future technologies," *Nature Reviews Drug Discovery*, vol. 1, no. 6, pp. 447-456, 2002.

[69] S. Eun Chung, J. Kim, D. Yoon Oh, et al., "One-step pipetting and assembly of encoded chemical-laden microparticles for high-throughput multiplexed bioassays," *Nature Communications*, vol. 5, no. pp. 2014.

[70] J. Zhu, "Bioactive modification of poly(ethylene glycol) hydrogels for tissue engineering," *Biomaterials*, vol. 31, no. 17, pp. 4639-4656, 2010.

[71] P. D. Drumheller, J. A. Hubbell, "Polymer networks with grafted cell adhesion peptides for highly biospecific cell adhesive substrates," *Analytical Biochemistry*, vol. 222, no. 2, pp. 380-388, 1994.

[72] S. Park, H. J. Lee, W.-G. Koh, "Multiplex immunoassay platforms based on shape-coded poly(ethylene glycol) hydrogel microparticles incorporating acrylic

acid," *Sensors*, vol. 12, no. 6, pp. 8426-8436, 2012.

[73] E. Cevher, E. Ş. Çağlar, A. D. Sezer. *Gene delivery systems: Recent progress in viral and non-viral therapy*. (2012).

[74] M. Martin-Fernandez, S. V. Longshaw, I. Kirby, et al., "Adenovirus type-5 entry and disassembly followed in living cells by fret, fluorescence anisotropy, and flim," *Biophysical Journal*, vol. 87, no. 2, pp. 1316-1327, 2004.

[75] P. N. Reynolds, D. T. Curiel, "New generation adenoviral vectors improve gene transfer by coxsackie and adenoviral receptor-independent cell entry," *Kidney International*, vol. 61, no. S1, pp. S24-S31, 2002.

[76] *Sulfo-nhs (n-hydroxysulfosuccinimide)*, <https://www.lifetechnologies.com/order/catalog/product/24510%3E>.

[77] W.-W. Hu, M. W. Lang, P. H. Krebsbach, "Development of adenovirus immobilization strategies for in situ gene therapy," *The Journal of Gene Medicine*, vol. 10, no. 10, pp. 1102-1112, 2008.

[78] *Avidin-biotin interaction*, <https://www.lifetechnologies.com/kr/ko/home/life-science/protein-biology/protein-biology-learning-center/protein-biology-resource-library/pierce-protein-methods/avidin-biotin-interaction.html%3E>.

[79] S. Fengler, P. H Bastiaens, H. Grecco, et al., "Optimizing cell arrays for accurate functional genomics," *BMC Research Notes*, vol. 5, no. 1, pp. 358, 2012.

[80] U. F. Greber, M. Willetts, P. Webster, et al., "Stepwise dismantling of adenovirus 2 during entry into cells," *Cell*, vol. 75, no. 3, pp. 477-486, 1993.

[81] M. Y. Nakano, K. Boucke, M. Suomalainen, et al., "The first step of adenovirus type 2 disassembly occurs at the cell surface, independently of endocytosis and escape to the cytosol," *Journal of Virology*, vol. 74, no. 15, pp. 7085-7095, 2000.

[82] M. W. Pandori, T. Sano, "Chemically inactivated adenoviral vectors that can efficiently transduce target cells when delivered in the form of virus-microbead conjugates," *Gene Therapy*, vol. 12, no. 6, pp. 521-533, 2005.

[83] I. Dmitriev, V. Krasnykh, C. R. Miller, et al., "An adenovirus vector with genetically modified fibers demonstrates expanded tropism via utilization of a

coxsackievirus and adenovirus receptor-independent cell entry mechanism," *Journal of Virology*, vol. 72, no. 12, pp. 9706-9713, 1998.

[84] R. Sullivan, J. Tierney, R. READ, "Thermal destruction of adenovirus 12, reovirus 1, and herpes simplex in milk," in *Journal of Dairy Science,* 1969, pp. 897-&.

[85] C. Granas, B. K. Lundholt, A. Heydorn, et al., "High content screening for g protein-coupled receptors using cell-based protein translocation assays," *Combinatorial Chemistry & High Throughput Screening*, vol. 8, no. 4, pp. 301-309, 2005.

[86] K. Liu, N. Southall, S. a. Titus, et al., "A multiplex calcium assay for identification of gpcr agonists and antagonists," *Assay and drug development technologies*, vol. 8, no. 3, pp. 367-379, 2010.

[87] W. Thomsen, J. Frazer, D. Unett, "Functional assays for screening gpcr targets," *Current Opinion in Biotechnology*, vol. 16, no. 6, pp. 655-665, 2005.

[88] B. R. Conway, L. K. Minor, J. Z. Xu, et al., "Quantification of g-protein coupled receptor internalization using g-protein coupled receptor-green fluorescent protein conjugates with the arrayscan™ high-content screening system," *Journal of Biomolecular Screening*, vol. 4, no. 2, pp. 75-86, 1999.

[89] A. Carpenter, T. Jones, M. Lamprecht, et al., "Cellprofiler: Image analysis software for identifying and quantifying cell phenotypes," *Genome Biology*, vol. 7, no. 10, pp. R100, 2006.

국문 초록

본 논문에서는 고속 다중변수 세포기반 분석을 위해 세포층에 패치형태로 사용가능한 아데노바이러스 벡터가 표면에 고정된 코드화된 마이크로입자를 개발하고, 이를 코드화된 바이러스 마이크로패치라 명명한다. 이 기술은 2 차원 모양으로 코드화된 바이러스 마이크로패치들의 혼합물을 2 차원 단일층으로 길러진 세포에 단순히 파이펫팅함으로써 아데노바이러스 벡터 기반의 유전자 전달을 공간적으로 제한한다. 이를 통해 무작위로 뿌려진 마이크로패치에 상응하게 서로 다른 감염된 세포군집들이 생성이 되고, 각 세포군집에 전달된 유전자의 종류는 마이크로패치의 모양에 의해 식별할 수 있다. 이를 위해, 모양으로 코드화된 고분자 마이크로입자들이 광리소그래피 방식으로 제작하였고, 그 표면에 아데노바이러스 벡터를 특이적으로 고정시킴으로써 고수준으로 지역화된 유전자 전달이 달성하였다. 이러한 특징은 표준 마이크로플레이트의 하나의 웰 안에서 복합화를 통한 고속 화합물 스크리닝을 가능케 하고 또한, 이미지 기반의 다중변수 분석기를 사용한 형광기반 분석형태에 적용을 위한

어떠한 제한점도 만들지 않는다. 이 기술의 역량을 보여주기 위해서 화합물 처리와 형광 이미징 기반으로 세포 이하 수준의 타겟 추적이 필요한 복합화된 G-protein coupled receptor (GPCR) 내재화 분석을 시행하였다.

먼저, 다양한 2 차원적 그래픽 코드를 갖는 마이크로입자의 제작을 위해 자동화된 스텝-앤-리핏 동작을 지원하는 마스크리스 리소그래피 시스템을 개발하였다. 이 시스템을 이용하여 위조약 방지, 복합화된 바이오 분석을 위한 작은 부피 액체의 병렬 적재, 그리고 백색 발광다이오드를 위한 형광체 균일 코팅 등의 코드화된 마이크로입자와 리소그래피 기술의 새로운 응용분야를 탐구하였다.

코드화된 바이러스 마이크로패치의 개발을 위해서는 다양한 모양으로 코드화된 마이크로입자를 제작하였고, 이 입자들의 표면은 아데노바이러스 벡터의 특이적 고정을 위해 카르복실기를 가지도록 하였다. 이러한 표면 기능화는 광경화 폴리머 용액에 아크릴산을 함유시킴으로써 달성되었다. 그 후, 제작된 마이크로입자 위에 아데노바이러스 벡터 고정을 위해 두 가지 방법을 개발하였다. 첫번째 방법은 마이크로입자 표면의 카르복실기와 아데노바이러스 표면 단백질에 존재하는 아민기를 1-ethyl-3-(3-dimethylaminopropyl)carbodiimide (EDC)와 N-hydroxysulfosuccinimide (Sulfo-NHS)를 이용하여 직접적으로 결합한다. 면역형광시험과 주사전자현미경 관찰을 통해 고정된 아데노바이러스 벡터를 확인하였다. 두번째 방법은 아비딘-바이오틴 작용을 활용한다. 이 방법에서는 마이크로입자와 아데노바이러스 벡터 표면이 각각 아민 활성화된 바이오틴과

아민 반응적 바이오틴으로 바이오틴화 되고, 후에 아비딘을 매개로 하여 연결된다. 이 방식을 통한 아데노바이러스 벡터의 고정도 주사전자현미경 관찰을 통해 확인하였다.

위 두가지 방식으로 제작된 코드화된 바이러스 마이크로패치들의 지역화된 유전자 전달을 표준 96-웰 마이크로 플레이트에서 길러진 인간 골수암 세포라인인 U-2 OS 의 감염 테스트를 통해 확인하였다. EDC/Sulfo-NHS 를 사용하여 제작된 첫번째 형태의 코드화된 바이러스 마이크로패치는 비특이적으로 고정된 아데노바이러스 벡터의 번짐으로 인해 저수준의 지역화된 유전자 전달을 달성하였다. 그러나, 아비딘-바이오틴 작용을 활용하여 제작한 코드화된 바이러스 마이크로패치는 고수준의 지역화된 유전자 전달을 보였다. 이러한 우수한 결과는 바이오틴화된 아데노바이러스 벡터의 바이러스 수용체 독립적인 감염에 기인하며, 이 사실은 아데노바이러스 수용체가 없는 세포라인의 감염 실험을 통해 심화 탐구하였다.

마지막으로, 코드화된 바이러스 마이크로패치를 기반으로 복합화된 GPCR 내재화 분석을 수행하였다. 고속 세포기반의 GPCR 기능 분석의 개발은 신약개발과정의 큰 화합물 라이브러리 스크리닝을 위해 매우 중요하며, 리간드에 유도된 수용체 내재화 분석은 여러가지 GPCR 분석법 중에서도 다양한 GPCR 종류에 광범위하게 적용 가능하다. 그러나, 이는 형광기반으로 세포내부에서 수용체 내재화를 측정하기 위해서 이미징 기반의 다중변수 분석이 필요하다. 이를 해결하기 위해서, 녹색형광단백질 유전자가 표지된 GPCR 유전자를 가지는

아데노바이러스 벡터들을 사용하여 세 가지 종류의 코드화된 바이러스 마이크로패치를 제작하였다. 이 마이크로패치들을 96-웰 마이크로 플레이트에 길러진 단일 세포층에 파이펫팅하여 동시에 여러가지 GPCR 들을 발현시킴으로써, 하나의 리간드에 대한 여러가지 GPCR 들의 반응을 하나의 공간에서 획득하였다. 마이크로패치 기반의 복합화된 실험은 자유로운 아데노바이러스 벡터를 사용하는 일반적인 단일화된 실험에 비해 유전자 전달와 리간드 전달을 위한 파이펫팅 횟수를 줄여주면서, 동일한 다중변수 분석법을 적용하여 같은 실험 결과를 얻을 수 있었다.

코드화된 바이러스 마이크로패치는 세포 마이크로어레이 생성을 대단히 간단하게 하며 이미지 기반의 다중변수 분석에 적합하므로, 신약개발을 위한 세포기반 분석을 가속화하고 강화할 것으로 예상한다.

주요어 : 세포기반 분석, 다중변수 스크리닝, 복합화, 바이러스 기반 유전자 전달, 코드화된 마이크로입자

학번 : 2010-20910